

Simplex path integral and renormalization group for high-order interactions*

Aohua Cheng,[†] Yunhui Xu,[‡] Pei Sun,[§] and Yang Tian[¶]

Modern theories of phase transitions and scale-invariance are rooted in path integral formulation and renormalization groups (RG). Despite the applicability of these approaches on simple systems with only pairwise interactions, they are less effective on complex systems with un-decomposable high-order interactions (i.e., interactions among arbitrary sets of units). To precisely characterize the universality of high-order interacting systems, we propose simplex path integral and simplex renormalization group (SRG) as the generalizations of classic approaches to arbitrary high-order and heterogeneous interactions. We first formalize the trajectories of units governed by high-order interactions to define path integrals on corresponding simplexes based on a high-order propagator. Then we develop a method to integrate out short-range high-order interactions in the momentum space, accompanied by a coarse graining procedure functioning on the simplex structure generated by high-order interactions. The proposed SRG, equipped with a divide-and-conquer framework, can deal with the absence of ergodicity arised from the sparse distribution of high-order interactions and renormalize a system with intertwined high-order interactions on p -order according to its properties on q -order ($p \leq q$). The associated scaling relation and its corollaries support to differentiate among scale-invariant, weak-scale-invariant, and scale-dependent systems across different orders. We have validated our theory in multi-order scale-invariance verification, organizational structure identification, and information bottleneck analysis to demonstrate its capacity for identifying intrinsic properties of high-order interacting systems during system reduction.

I. INTRODUCTION

A. Unknowns about high-order interactions

Over the past decades, the studies on phase transition phenomena, especially the non-equilibrium ones, in different interacting systems have accomplished substantial progress [1, 2]. This progress should be credited to the development of path integral [3–5] and renormalization group [6, 7] theories, which significantly deepen our understanding of system dynamics and provide a precise formulation of scaling and criticality.

However, a non-negligible theoretical vacancy can be found in the existing path integral and renormalization group approaches if we subdivide interactions into pairwise and high-order categories. As the name suggests, a pairwise interaction only involves a pair of units and does not require the participation of any other unit. This kind of interaction can be represented by edges in networks [8, 9] and are implicitly used in the derivations of classic path integrals and renormalization groups (e.g., see Ref. [10]). A high-order interaction, on the contrary, is the mutual coupling among more than two units [11–13]. While some high-order interactions are

reducible and can be decomposed into a group of pairwise interactions, most high-order interactions are un-decomposable and in-equivalent to the direct sum of the pairwise ones [9, 14]. For instance, the triplet collaboration among three agents is not equivalent to the trivial sum of three pairs of individual collaborations. These un-decomposable high-order interactions have intricate effects on system dynamics [13, 14] and can not be trivially represented by ordinary networks [12]. Although notable efforts have been devoted to studying the optimal characterization of high-order interactions (e.g., using simplicial complexes [15–18] or hypergraphs [19–21]), there are fewer works focusing on developing specialized path integral and renormalization group theories for complex systems with high-order interactions [17, 22]. The difficulty of proposing these specialized frameworks arises from the intrinsic dependence on pairwise interactions when researchers constrain the discrete replicas of interacting systems as conventional networks. Once this constraint is relaxed, the intertwined effects of newly included high-order interactions would make the analysis on emerging dynamics highly non-trivial and even lead to novel results that can not be directly derived by classic theories (e.g., see instances in diffusion and random walks [16, 20, 23], social dynamics [24–26], and neural dynamics [27, 28]).

B. Related works and remaining challenges

To suggest a possible direction for developing path integral and renormalization group theories for high-order interactions, we summarize the accomplishments and limitations of previous works.

To date, most progress of the computational implementations of path integrals and renormalization groups

* Correspondence should be addressed to Y.T and P.S.

[†] aohuacheng18@gmail.com; Tsien Excellence in Engineering Program, Tsinghua University, Beijing, 100084, China.

[‡] yhxu0916@gmail.com; Department of Physics, Tsinghua University, Beijing, 100084, China.

[§] peisun@tsinghua.edu.cn; Department of Psychology & Tsinghua Laboratory of Brain and Intelligence, Tsinghua University, Beijing, 100084, China.

[¶] tiany20@mails.tsinghua.edu.cn & tyanyang04@gmail.com; Department of Psychology & Tsinghua Laboratory of Brain and Intelligence, Tsinghua University, Beijing, 100084, China.

is achieved on real systems with pairwise interactions [10, 29–33]. Although box-covering methods [34–37] may be the most straightforward ways for coarse graining while preserving the organizational properties of a system represented by a network, they depend on the assumption of internal fractal properties and convey no information about system dynamics. Different from box-covering, spectral method [38] pays more attention to inherent dynamics properties (e.g., random walks) during coarse graining but may suffer from the obstacles of finding super-units implied by small-world effects [10, 33, 39]. Aiming at resolving the coexisting and correlated scales, a geometric renormalization group is developed to identify the potential geometric scaling rather than path-distance scaling [33]. Nevertheless, this approach essentially relies on the *a-priori*-knowledge of the hidden metric space of networks (e.g., the hyperbolic space [40]). With the pursuit of realizing the metric-free coarse graining whose iterability is not limited by small-world effects, a Laplacian renormalization group (LRG) [10] has been derived from the diffusion on networks, a continuum counterpart of the block-spin transformation [41], to deal with the network topology, dynamics, and geometry encoded by the graph Laplacian operator [42]. This approach has a natural connection with path integrals as well [43]. Although these properties make the LRG a promising foundation for in-depth explorations, this framework suffers from several non-negligible limitations. First, there is no apparent correspondence between the LRG and an appropriate approach for analyzing undecomposable high-order interactions because the Laplacian operator can not characterize polyadic relations directly [9, 11–14]. Second, the intrinsic dependence of the LRG on the ergodic property of system dynamics reflected by network connectivity limits the applicability of this approach in analyzing high-order interactions, which are more sparsely distributed in the system than pairwise interactions and do not necessarily ensure ergodicity.

There exist fewer pioneering works devoted to developing renormalization groups for high-order interactions, among which, a notable framework is the real space renormalization group proposed by Refs. [17, 22]. This approach is initially defined on the Laplacian operators of the network skeletons of the Apollonian [44] and the pseudo-fractal [45] simplicial complexes to calculate spectral dimensions [22]. Then, it is generalized to the normalized up-Laplacian operator [16, 23] of simplicial complexes to deal with high-order spectra. Despite the effectiveness of this approach, its dependence on the non-trivial manual derivations using the Gaussian model [46] and the specialized application scope about spectral dimensions [17, 22] make it less applicable to the real scenarios where a programmatic implementation is demanded for renormalizing the complex systems generated by empirical data automatically.

In sum, while representative works such as the LRG [10] have suggested a promising way to renormalize complex systems, the appropriate path integral and renor-

malization group theories for high-order interactions remain clouded by numerous theoretical unknowns and technical difficulties.

C. Our frameworks and contributions

To fill these gaps, we generalize classic path integral and renormalization group theories from dyadic to polyadic relations. To realize such generalizations, we are required to derive the appropriate definitions of the canonical density operators (i.e., the functional over fields) [10, 49, 50] and the coarse graining processes in real and moment spaces [6, 7] for high-order interactions.

Our work suggests a possible way to define these concepts on simplexes, in which simplexes can join any subset of units to characterize un-decomposable high-order interactions among them (see Fig. 1(a) for instances). We propose two kinds of high-order propagators as the generalized path integral formulation of the abstract diffusion processes driven by multi-order interactions, which further creates a system mode description tantamount to the moment space. The coarse graining in the moment space is implemented by progressively integrating out short-range system modes corresponding to some certain order of interactions. Parallel to this process, we propose a real space coarse graining procedure to reduce the simplex structures associated with short-range high-order interactions, where we suggest a way to overcome the dependence on ergodicity. The correspondence between the moment and real spaces enables our framework to the system coarse graining according to both organizational structure and internal dynamics. Taken together, these definitions give birth to our simplex path integral and simplex renormalization group (SRG) theories, which are applicable to arbitrary orders of interactions.

The SRG can be used to uncover the potential scale invariance of high-order interactions, whose non-trivial fixed point may suggest the existence of critical phenomena. Different from conventional renormalization groups, the SRG is designed to renormalize p -order interactions in the system according to the structure and dynamics associated with q -order interactions ($p \leq q$). Therefore, we can compare the renormalization flow of p -order interactions guided by p -order interactions with that guided by arbitrary higher-order interactions. This feature allows us to investigate the impacts of higher-order interactions on lower-order ones and study the differences between lower-order and higher-order interactions in terms of scaling properties. In a special case with $p = q = 1$ (i.e., pairwise interactions), the two kinds of high-order propagators developed in our work both reduce to the classic counterpart used in the LRG [10] and our proposed SRG can reproduce the outputs of the LRG in the ergodic case.

To demonstrate the capacity of our approaches in identifying the latent characteristics of diverse real complex

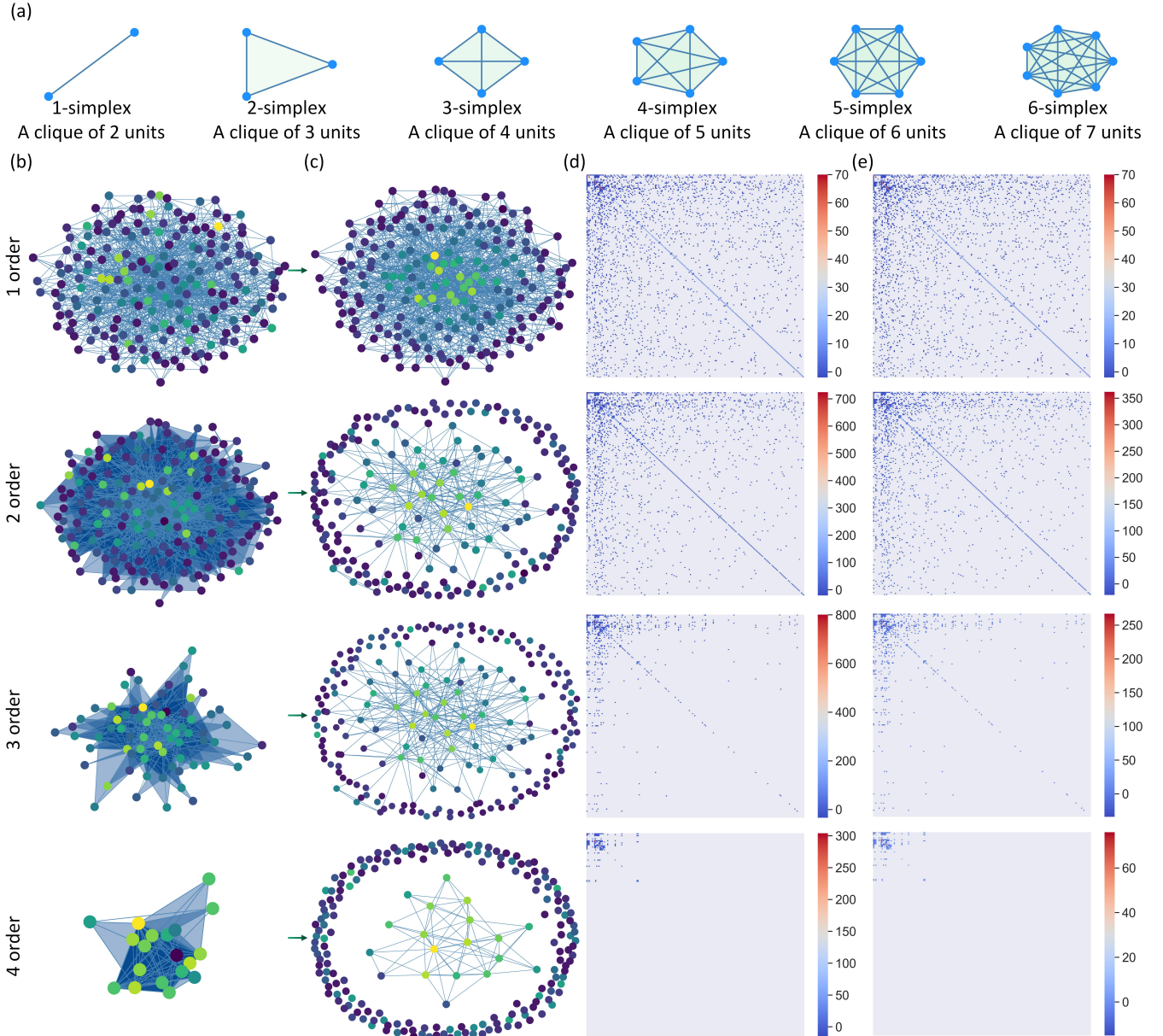


FIG. 1. System evolution governed by high-order interactions. (a) The simplicial complexes of different orders are presented. A n -order simplex manifests itself as a clique with $n+1$ units in the network. The 1-order simplex is equivalent to a pairwise interaction. (b) An instance of the interacting system with high-order interactions is presented, where there are 200 units whose pairwise interactions follow a Barabási-Albert network (the number of edges to attach from a new node to existing nodes is set as $c = 6$) [47, 48]. The units engaged with the first four orders of interactions are extracted using simplicial complexes. (c) The associated network sketches of the system shown in (b) are presented on each order, where two units share an edge in the network sketch on n -order only if they are engaged with a n -order interaction in the system. (d-e) The corresponding multi-order Laplacian (d) and high-order path Laplacian (e) operators of the system shown in (b) are illustrated in every order.

systems, we validate our framework from the perspectives of multi-order scale-invariance detection, latent organizational structure identification, and information bottleneck optimization, respectively. An efficient code implementation of this framework is provided in [51].

II. UN-DECOMPOSABLE HIGH-ORDER INTERACTIONS

The Laplacian operator is a natural choice for characterizing interactions and their spreading among units [52–54]. In a special case with pairwise interactions, the Laplacian has a classic expression, $\mathbf{L}_{ij} = \delta_{ij} \sum_k \mathbf{A}_{ik} - \mathbf{A}_{ij}$, where δ denotes the Kronecker delta function and

\mathbf{A} is a weighted adjacency matrix that describes the non-negative coupling strengths among all units in unit set V (here the non-negativity is required by the Laplacian). Under the autonomous condition, the evolution of system dynamics given an initial state \mathbf{x}_0 is defined by $\mathbf{x} = \exp(-\tau \mathbf{L}) \mathbf{x}_0$, where $\tau \in (0, \infty)$ denotes a time scale [55]. However, in more general cases with undecomposable high-order interactions, the classic Laplacian operator is no longer applicable. To fill the gap, previous studies have explored the generalization of the Laplacian operator on uniform hypergraphs [56, 57] and simplicial complexes [9, 23, 58, 59], where diverse variants of the Laplacian (e.g., the Hodge Laplacian [23] and the multi-order Laplacian [9]) have been proposed to characterize high-order interactions. In our work, we first derive a multi-order Laplacian following the spirit of Ref. [9]. Then we develop a new operator, referred to as the high-order path Laplacian, as an alternative description of high-order interactions.

A. High-order interactions through faces

Let us consider the n -order interactions that manifest as the simultaneous participation of $n+1$ related units. The un-decomposability of these interactions lies in that the couplings among $n+1$ units are required to occur simultaneously and none of them is dispensable. For instance, the triplet collaboration requires the participation of all three agents together. As discussed in Ref. [9], these interactions can be represented by the n -faces of the n -simplex where $n+1$ units are placed on. For the sake of clarity, we define $\{i\}_{n+1} \subset V$ as an arbitrary set of $n+1$ units in which unit i is included and denote $S_{n+1}^{\{i\}}$ as the set of all permutations (i.e., rearrangements) on $\{i\}_{n+1}$. The multi-order Laplacian $\mathbf{L}_M^{(n)}$ associated with n -simplexes is defined as

$$[\mathbf{L}_M^{(n)}]_{ij} = n\delta_{ij}\mathbf{D}_i^{(n)} - \mathbf{A}_{ij}^{(n)}. \quad (1)$$

In Eq. (1), term $\mathbf{D}_i^{(n)}$ counts the number of n -simplexes that contains unit i

$$\mathbf{D}_i^{(n)} = \frac{1}{(n+1)!} \sum_{\{i\}_{n+1} \subset V} \prod_{\omega \in S_{n+1}^{\{i\}}} \mathbf{M}_\omega, \quad (2)$$

where $\frac{1}{(n+1)!}$ serves the normalization for high-order simplexes (i.e., the enumeration in Eq. (2) involves repetition in high-order cases). Term $\mathbf{A}_{ij}^{(n)}$ counts the number of n -simplexes that contains units i and j

$$\mathbf{A}_{ij}^{(n)} = \frac{1 - \delta_{ij}}{(n+1)!} \sum_{\{i,j\}_{n+1} \subset V} \prod_{\omega \in S_{n+1}^{\{i,j\}}} \mathbf{M}_\omega, \quad (3)$$

where $\{i,j\}_{n+1} \subset V$ is an arbitrary set of $n+1$ units in which units i and j are included. The general definition

of \mathbf{M}_ω used in Eq. (2-3) is given as a product of a series of matrices for any permutation $\omega = (k_1 \dots k_n)$

$$\mathbf{M}_\omega = \mathbf{A}_{k_1 k_2} \cdots \mathbf{A}_{k_{n-1} k_n}, \quad (4)$$

where $\mathbf{A} = \mathbf{A}^{(1)}$ is the classic adjacency matrix of units.

In Eq. (2), vector $\mathbf{D}^{(n)}$ is similar to the degree vector while matrix $\mathbf{A}^{(n)}$ can be understood as the adjacency matrix. In a special case where $n = 1$, Eq. (2) is equivalent to the classic Laplacian for pairwise interactions. In the more general cases where $n > 1$, high-order interactions can be characterized by Eq. (2). Please see Fig. 1(d) for the illustrations of the multi-order Laplacian. Although the definitions of Eqs. (2-4) are different from the approach proposed by Ref. [9], they are mathematically consistent with Ref. [9].

B. High-order interactions along paths

Then, we turn to another type of n -order interactions, which manifest as the sequential actions of $n+1$ related units after they all participate in. The un-decomposability of these interactions arises from that the mutual coupling effects emerge only after $n+1$ units have been engaged with the interplay progressively. For example, a pipeline-like collaboration may require all agents to communicate with each other and behave in order. Each previous action is globally known to all agents and affects all subsequent actions. This property can be characterized by the paths (i.e., a sequence of 1-simplexes) that successively pass through the $n+1$ units placed on the n -simplex. To describe the interactions propagating along the paths on n -simplexes, we develop an operator named as the high-order path Laplacian $\mathbf{L}_H^{(n)}$

$$[\mathbf{L}_H^{(n)}]_{ij} = \frac{1}{n} \left(\delta_{ij} \mathbf{P}_i^{(n)} - \mathbf{B}_{ij}^{(n)} \right). \quad (5)$$

In Eq. (5), coefficient $\frac{1}{n}$ denotes the normalization of the propagation speed of interactions along paths. Term $\mathbf{P}_i^{(n)}$ counts the number of paths that traverse all $n+1$ units on the n -simplex without repetition and terminate at unit i

$$\mathbf{P}_i^{(n)} = \frac{1}{n+1} \sum_{\{i\}_{n+1} \subset V} \prod_{\omega \in S_{n+1}^{\{i\}}} \mathbf{M}_\omega, \quad (6)$$

where $\frac{1}{n+1}$ denotes the normalization. Term $\mathbf{B}_{ij}^{(n)}$ counts the number of paths that traverse all $n+1$ units on the n -simplex without repetition, initiate at unit j , and terminate at unit i

$$\mathbf{B}_{ij}^{(n)} = \frac{1 - \delta_{ij}}{n(n+1)} \sum_{\{i,j\}_{n+1} \subset V} \prod_{\omega \in S_{n+1}^{\{i,j\}}} \mathbf{M}_\omega. \quad (7)$$

Please see Fig. 1(e) for the instances of the high-order path Laplacian. In the case with $n = 1$, Eqs. (6-7)

reduce to the classic degree vector and adjacency matrix, respectively (i.e., we have $\mathbf{P}^{(1)} = \mathbf{D}^{(1)}$ and $\mathbf{B}^{(1)} = \mathbf{A}$). Therefore, Eq. (5) denotes the classic Laplacian when interactions are pairwise.

In general, one can choose the multi-order Laplacian $\mathbf{L}_M^{(n)}$ and the high-order path Laplacian $\mathbf{L}_H^{(n)}$ according to application demands. While $\mathbf{L}_M^{(n)}$ conveys information about the high-order interactions that units are simultaneously engaged with, the definition of $\mathbf{L}_H^{(n)}$ is more applicable to the cases where a high-order interaction is formed by an irreducible sequence of the participation of related units. We offer efficient code implementations of these two kinds of operators, which can be seen in Ref. [51]. For convenience, we uniformly denote them as $\mathbf{L}^{(n)}$ in our subsequent derivations. One can specify the actual definition of $\mathbf{L}^{(n)}$ in the application.

III. SIMPLEX PATH INTEGRAL

Given the high-order interactions described by $\mathbf{L}^{(n)}$, we turn to explore the path integral formulation of the trajectories of units governed by high-order interactions. As first suggested by Ref. [42] and then discussed in Refs. [10, 43, 60–62], the Laplacian can be understood as a Hamiltonian if we consider the system dynamics governed by it. In the case of high-order interactions, we can consider the eigendecomposition, $\mathbf{L}^{(n)} = \sum_{\lambda^{(n)}} \lambda^{(n)} |\lambda^{(n)}\rangle\langle\lambda^{(n)}|$, using the bra-ket notation and define a time evolution operator

$$\mathbf{U}_\tau^{(n)} = \exp(-\tau \mathbf{L}^{(n)}) \quad (8)$$

$$= \sum_{k=0}^{\infty} \frac{1}{k!} (-\tau \mathbf{L}^{(n)})^k, \quad (9)$$

$$= \sum_{\lambda^{(n)}} \exp(-\tau \lambda^{(n)}) |\lambda^{(n)}\rangle\langle\lambda^{(n)}|. \quad (10)$$

As suggested by Eq. (9), this operator characterizes the probability for each unit to evolve from one state to another state within a given time scale τ , i.e., $|\mathbf{x}\rangle = \mathbf{U}_\tau^{(n)} |\mathbf{x}_0\rangle$. The characterization is realized by considering the distributions of units, $\frac{(-\tau \mathbf{L}^{(n)})^k}{k!}$, generated by all the possible ways of evolution, $k \in (0, \infty)$, during a time period of τ . See Fig. 2(a) for illustrations. As indicated by Eq. (10), the probability amplitude is intrinsically determined by the exponential decay rates of diffusion modes in a moment space. Short-range interactions associated with fast decays (i.e., large eigenvalues) in the moment space have small impacts on units.

At equilibrium, the Gibbs state of the system associated with n -order interactions is

$$\rho^{(n)} = \frac{\mathbf{U}_\tau^{(n)}}{\text{tr}(\mathbf{U}_\tau^{(n)})} = \frac{\sum_{\lambda^{(n)}} \exp(-\tau \lambda^{(n)}) |\lambda^{(n)}\rangle\langle\lambda^{(n)}|}{\sum_{\lambda^{(n)}} \exp(-\tau \lambda^{(n)})}, \quad (11)$$

where $\text{tr}(\cdot)$ denotes the trace and parameter τ serves as the inverse of a finite temperature. Please see Fig. 2(b) for instances. The Boltzmann constant is assumed as unitary for simplicity. The partition function, $\sum_{\lambda^{(n)}} \exp(-\tau \lambda^{(n)})$, is proportional to the average return probability of random walks within a time scale τ [42]. See Figs. 2(b-c) for illustrations.

Eq. (11) defines a density operator of system evolution characterized by high-order interactions

$$\langle \mathbf{x} | \rho^{(n)} | \mathbf{x}_0 \rangle = \frac{1}{\text{tr}(\mathbf{U}_\tau^{(n)})} \langle \mathbf{x} | \mathbf{U}_\tau^{(n)} | \mathbf{x}_0 \rangle, \quad (12)$$

which naturally relates to the path integral formulation. Let us consider a minimum time step ε such that $N = \frac{\tau}{\varepsilon}$. At the limit $N \rightarrow \infty$ (or $\varepsilon \rightarrow 0$), the numerator of the density operator (i.e., the time evolution operator) implies a power form of the corresponding high-order propagator $\mathbf{K}^{(n)}(\mathbf{x}, \mathbf{x}_0, \tau) = \langle \mathbf{x} | \mathbf{U}_\tau^{(n)} | \mathbf{x}_0 \rangle = \lim_{N \rightarrow \infty} \langle \mathbf{x} | \left(\mathbf{U}_\varepsilon^{(n)} \right)^N | \mathbf{x}_0 \rangle$. On the one hand, this power form expression directly leads to a path integral in conventional quantum field theory

$$\begin{aligned} & \mathbf{K}^{(n)}(\mathbf{x}, \mathbf{x}_0, \tau) \\ &= \lim_{N \rightarrow \infty} \int \prod_{k=0}^{N-1} \langle \mathbf{x}_{(k+1)\varepsilon} | \mathbf{U}_\varepsilon^{(n)} | \mathbf{x}_{k\varepsilon} \rangle d\mathbf{x}_\varepsilon \cdots d\mathbf{x}_{(N-1)\varepsilon}, \end{aligned} \quad (13)$$

where we mark $\mathbf{x} = \mathbf{x}_{N\varepsilon}$. On the other hand, this power form expression can also be reformulated using the imaginary time and Eqs. (8-9)

$$\mathbf{K}^{(n)}(\mathbf{x}, \mathbf{x}_0, \tau) = \sum_{k=0}^{\infty} \frac{1}{k!} \left\langle \mathbf{x} \left| \left(-\frac{i}{\hbar} \int_0^\tau -i\hbar \mathbf{L}^{(n)} d\varepsilon \right)^k \right| \mathbf{x}_0 \right\rangle, \quad (14)$$

where notion \hbar denotes the Dirac constant. Eq. (14) is related to the imaginary time evolution governed by $\mathbf{L}^{(n)}$ in the infinite-dimensional path space. Specifically, the probability amplitude for the system to evolve from $|\mathbf{x}_0\rangle$ to $|\mathbf{x}\rangle$ during a period of τ conveyed by the propagator in Eq. (13) can be measured by summing over all possible evolution paths connecting between these two states (i.e., the discrete counterpart of path integrals) in Eq. (14). This is the reason why the network topology conveyed by $\mathbf{L}^{(n)}$ intrinsically shapes path integrals.

Moreover, the denominator of the density operator (i.e., the partition function) can be interpreted by con-

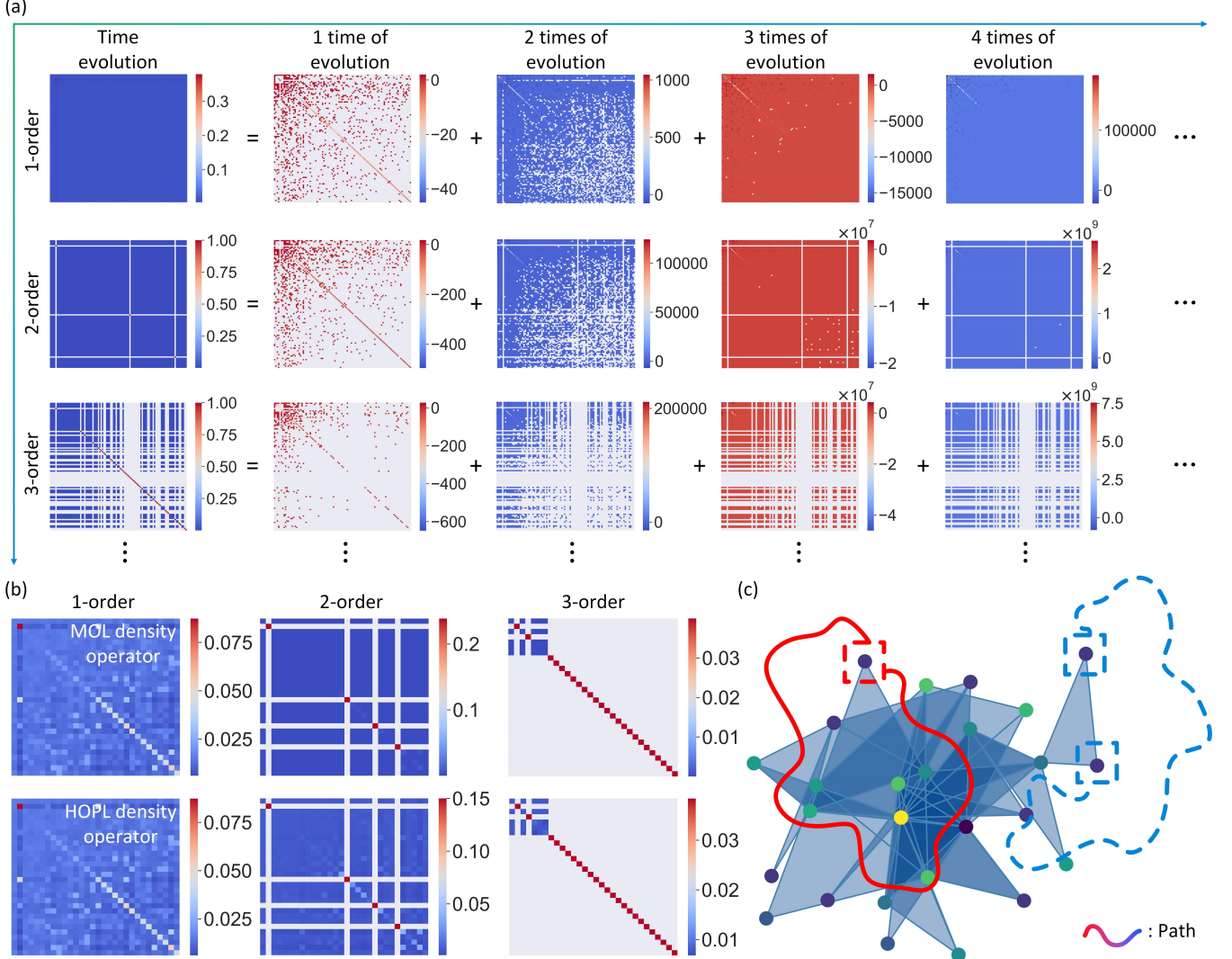


FIG. 2. Illustrations of the simplex path integral. (a) An interacting system of 100 units is generated, where the pairwise interactions of units follow a Barabási-Albert network ($c = 6$). This system is used to show the derivation of the time evolution operators of the first three orders, where we use the multi-order Laplacian (MOL) for calculation and set $\tau = 1$. For each order of interactions, we illustrate the first four terms of the series expansion of time evolution operator in Eq. (5). (b) For the system defined in (a), we show the density operators calculated based on the MOL or the high-order path Laplacian (HOPL) on each order. (c) We show that values in the density operator can be related to the evolution paths of system states. The blue path leads from one state to another while the red path starts from and ends at the same state.

sidering the expectation $\langle \mathbf{U}_\tau^{(n)} \rangle = \text{tr} (\rho^{(n)} \mathbf{U}_\tau^{(n)})$

$$\begin{aligned} & \text{tr} (\rho^{(n)} \mathbf{U}_\tau^{(n)}) \\ &= \int \langle \mathbf{x}_0 | \mathbf{U}_\tau^{(n)} | \mathbf{x}_0 \rangle d\mathbf{x}_0, \end{aligned} \quad (15)$$

$$= \int \left\langle \mathbf{x}_0 \left| \left(\oint_{\Gamma} \exp \left(-\frac{i}{\hbar} \int_0^\tau -i\hbar \mathbf{L}^{(n)} d\mathbf{x}_\varepsilon \right) d\mathbf{x}_\varepsilon \right) \right| \mathbf{x}_0 \right\rangle d\mathbf{x}_0, \quad (16)$$

where Γ is an arbitrary closed curve that starts from and ends at \mathbf{x}_0 . Eq. (16) suggests why the partition function is proportional to the average return probability of ran-

dom walks within a time scale τ from the perspective of path integral formulation. See Fig. 2(c) for illustrations.

The path integrals in Eqs. (13-16) are fully characterized by $\mathbf{L}^{(n)}$, which describes latent simplex structures of the system. They are integrals over all the possible evolution paths of a system governed by high-order interactions. Consequently, they are referred to as simplex path integrals in our work.

IV. SIMPLEX RENORMALIZATION GROUP

The connection between Eqs. (8-16) and the moment space naturally inspires us to consider the generalization

of renormalization groups. The freedom degrees corresponding to short-range interactions (e.g., fast diffusion within the clusters of strongly correlated units) can be safely coarse grained without significant information loss, which is consistent with our interpretation of Eq. (10). Here we develop a framework to generalize renormalization groups to high-order interactions, where we also propose possible ways to overcome the limitations of the Laplacian renormalization group (LRG) [10].

A. Renormalization procedure

To offer a clear vision, we first introduce our approach, referred to as the simplex renormalization group (SRG), in an ergodic case as assumed by Ref. [10]. The SRG renormalizes p -order interactions according to the properties of q -order interactions ($p \leq q$). Specifically, the renormalization is realized as the following:

- (1) In each k -th iteration, we have two iterative Laplacian operators, $\mathbf{L}_k^{(p)}$ and $\mathbf{L}_k^{(q)}$, and their associated high-order network sketches, $\mathbf{G}_k^{(p)}$ and $\mathbf{G}_k^{(q)}$, with $N_k^{(p)} = N_k^{(q)}$ units (there is an edge connecting between two units in $\mathbf{G}_k^{(p)}$ or $\mathbf{G}_k^{(q)}$ only if they share a p - or q -order interaction). A q -order density operator, $\rho_k^{(q)}$, is derived based on $\mathbf{L}_k^{(q)}$.
- (2) A parameter $n_k^{(q)}$ is defined as the number of the eigenvalues of $\mathbf{L}_k^{(q)}$ that are smaller than $\frac{1}{\tilde{\tau}^{(q)}}$, where $\tilde{\tau}^{(q)}$ is the time scale for q -order simplicial complexes (see Sec. IV B for the selection of $\tilde{\tau}^{(q)}$). These $n_k^{(q)}$ eigenvalues correspond to long-range high-order interactions because the contributions of their eigenvectors have slow decays in Eq. (10). Other eigenvalues correspond to short-range high-order interactions and can be coarse grained.
- (3) In the moment space, the current q -order Laplacian, $\mathbf{L}_k^{(q)}$, is reduced to the re-scaled contributions of the eigenvectors associated with long-range high-order interactions

$$\mathbf{Q}_k^{(q)} = \sum_{\lambda_k^{(q)}} \Theta \left(\frac{1}{\tilde{\tau}^{(q)}} - \lambda_k^{(q)} \right) \lambda_k^{(q)} |\lambda_k^{(q)}\rangle \langle \lambda_k^{(q)}|, \quad (17)$$

where $\Theta(\cdot)$ is the Heaviside step function (i.e., $\Theta(x) = 1$ if $x \geq 0$ and $\Theta(x) = 0$ if $x < 0$). Meanwhile, the current p -order Laplacian, $\mathbf{L}_k^{(p)}$, is reduced to the contributions of the $n_k^{(q)}$ smallest eigenvalues (i.e., long-range p -order interactions)

$$\mathbf{Q}_k^{(p)} = \sum_{\omega_k^{(p)}} I_{\Omega_k^{(p)}} \left(\omega_k^{(p)} \right) \omega_k^{(p)} |\omega_k^{(p)}\rangle \langle \omega_k^{(p)}|, \quad (18)$$

where $\Omega_k^{(p)}$ denotes the set of the $n_k^{(q)}$ smallest eigenvalues of $\mathbf{L}_k^{(p)}$ and $I_A(\cdot)$ is the indicator function defined on an arbitrary set A . Please note that the eigenvalues in $\Omega_k^{(p)}$ are not necessarily smaller than $\frac{1}{\tilde{\tau}^{(q)}}$.

- (4) In the real space, we generate $\mathbf{H}_k^{(q)}$, a copy of $\mathbf{G}_k^{(q)}$. Then we progressively remove the edges in $\mathbf{H}_k^{(q)}$ that correspond to small values in $\rho_k^{(q)}$ until there exist $n_k^{(q)}$ clusters in $\mathbf{H}_k^{(q)}$. Each cluster contains a set of strongly correlated units with short-range high-order interactions. In $\mathbf{G}_k^{(q)}$, each set of units that belong to the same cluster in $\mathbf{H}_k^{(q)}$ are aggregated into a super-unit to generate a new network $\mathbf{G}_{k+1}^{(q)}$. Consequently, there remain $n_k^{(q)}$ super-units in $\mathbf{G}_{k+1}^{(q)}$ after coarse graining. Parallel to this process, we also aggregate the units belonging to the same cluster of $\mathbf{H}_k^{(q)}$ into a super-unit in $\mathbf{G}_k^{(p)}$. The generated $\mathbf{G}_{k+1}^{(p)}$ contains $n_k^{(q)}$ super-units as well.
- (5) The correspondence between the moment space and the real space for q -order interactions is ensured by a candidate Laplacian $\mathbf{F}_{k+1}^{(q)}$. This operator is generated following $\left(\mathbf{F}_{k+1}^{(q)} \right)_{\nu_i \nu_j} = \langle \nu_i | \mathbf{Q}_k^{(q)} | \nu_j \rangle$, where ν_i and ν_j are super-units in $\mathbf{G}_{k+1}^{(q)}$. Notion $|\nu_j\rangle$ is a $N_k^{(q)}$ -dimensional ket where unitary components correspond to all the units in $\mathbf{G}_k^{(q)}$ that are aggregated in ν_i and zero components correspond to all other units in $\mathbf{G}_{k+1}^{(q)}$ that are not covered by ν_i . Mathematically, this procedure actually defines a similarity transformation T between $\mathbf{Q}_k^{(q)}$ and $\mathbf{F}_{k+1}^{(q)}$

$$T^{-1} \mathbf{Q}_k^{(n)} T = \text{diag} \left(\left[\mathbf{F}_{k+1}^{(n)}, \mathbf{0} \right] \right), \quad (19)$$

where $\mathbf{0}$ is a $(N_k^{(n)} - n_k^{(n)})$ -dimensional all-zero square matrix. It is clear that the similarity transformation is given as $T = \left(|\nu_1\rangle, \dots, |\nu_{n_k^{(n)}}\rangle, |\eta_{n_k^{(n)}+1}\rangle, \dots, |\eta_{N_k^{(n)}}\rangle \right)$, where each ket η_j is selected such that the columns of T define a group of orthonormal bases. Similarly, we can derive the candidate Laplacian $\mathbf{F}_{k+1}^{(p)}$ for p -order interactions based on $\mathbf{Q}_k^{(p)}$.

- (6) We re-scale candidate operators, $\mathbf{F}_{k+1}^{(p)}$ and $\mathbf{F}_{k+1}^{(q)}$, to derive the actual Laplacian of the coarse grained high-order systems as $\mathbf{L}_{k+1}^{(p)} = \chi^{(p)} \mathbf{F}_{k+1}^{(p)}$ and $\mathbf{L}_{k+1}^{(q)} = \chi^{(q)} \mathbf{F}_{k+1}^{(q)}$, where $\chi^{(p)} = \tilde{\omega}_k^{(p)} / \tilde{\omega}_{k+1}^{(p)}$ and $\chi^{(q)} = \tilde{\lambda}_k^{(q)} / \tilde{\lambda}_{k+1}^{(q)}$ are the re-scaling coefficients. Here $\tilde{\omega}_k^{(p)}$ and $\tilde{\omega}_{k+1}^{(p)}$ denote the smallest non-zero eigenvalues of $\mathbf{L}_k^{(p)}$ and $\mathbf{F}_{k+1}^{(p)}$, respectively. We set

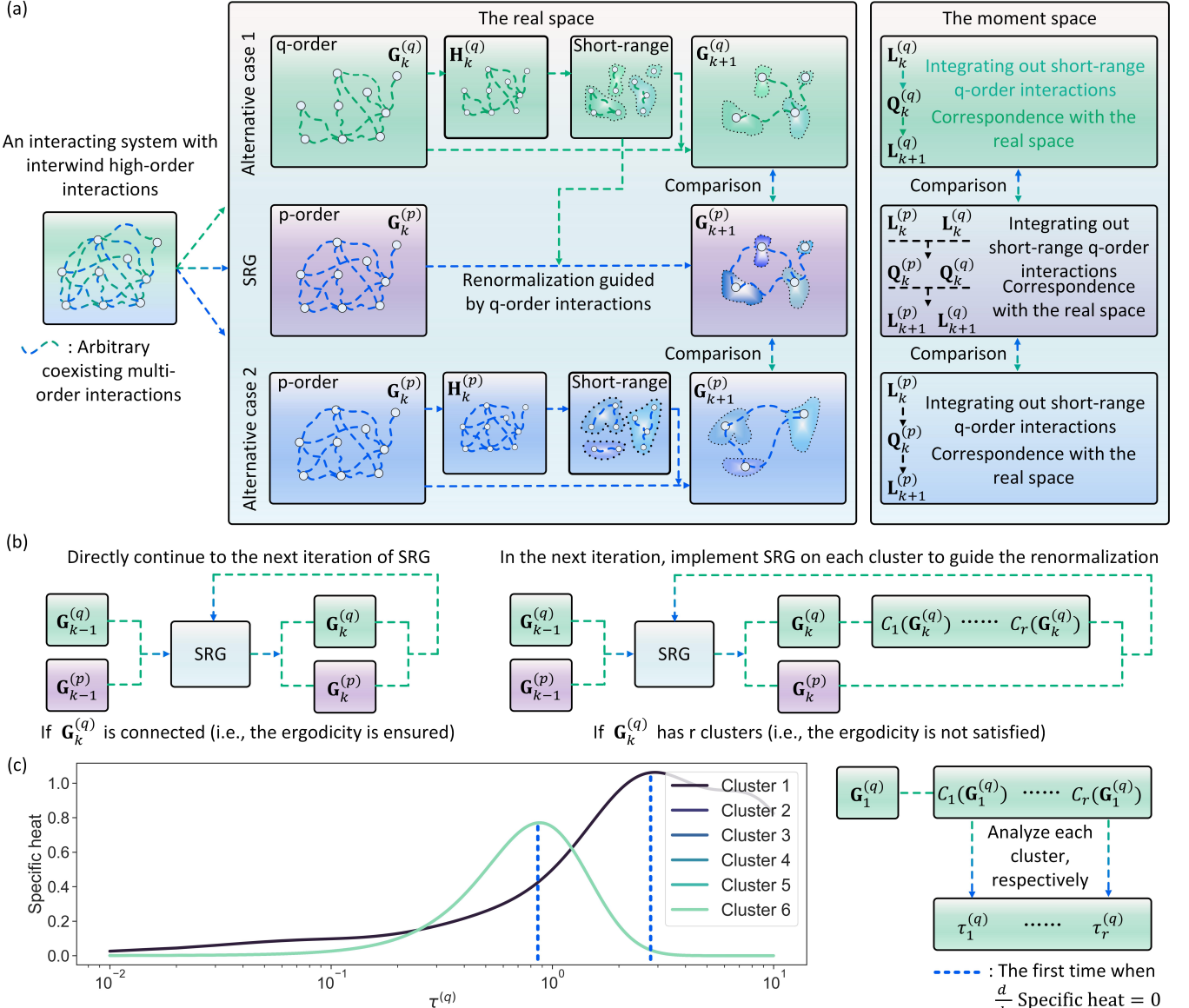


FIG. 3. Illustrations of the simplex renormalization group (SRG). (a) The conceptual illustration of the SRG is presented. For the sake of legibility, the simplicial complexes of different orders are not elaborated and are abstractly represented by dashed lines with different colors. Given a system where multi-order interactions coexist, the SRG can be applied to renormalize the system on the p -order based on the structure and dynamics associated with q -order interactions ($p \leq q$). (b) Conceptual illustrations of our divide-and-conquer procedure for dealing with the dependence of renormalization flows on the ergodicity. (c) A system with 500 units is defined, where pairwise interactions follow a Barabási-Albert network ($c = 2$). We use this system to illustrate the selection of time scale $\tau^{(q)}$ based on the specific heat ($q = 2$).

$\tilde{\lambda}_k^{(q)}$ and $\tilde{\lambda}_{k+1}^{(q)}$ as the smallest non-zero eigenvalues of $\mathbf{L}_k^{(q)}$ and $\mathbf{F}_{k+1}^{(q)}$. The derived $\mathbf{L}_{k+1}^{(p)}$ and $\mathbf{L}_{k+1}^{(q)}$ are used in the $(k+1)$ -th iteration.

After renormalizing $\mathbf{L}_k^{(p)}$ by repeating steps (1-6), the SRG progressively drives the system towards an intrinsic scale of p -order interactions that exceeds the microscopic scales. The renormalization of p -order interactions in both the real and moment spaces is realized under the guidance of q -order interactions (e.g., see steps (3-4) for

details). See Fig. 3(a) for a summary of key steps in our approach. Note that we use $\chi^{(p)}$ rather than $\tau^{(p)}$ as the re-scaling coefficient in step (3), which is slightly different from the re-scaling by τ in Ref. [10]. This re-scaling ensures that the minimum effective fluctuation rate (i.e., the minimum positive eigenvalue) in $\mathbf{L}_k^{(p)}$ becomes unitary in $\mathbf{L}_{k+1}^{(p)}$. Moreover, the using of a copy in step (4) is not necessary for theoretical derivations, yet it is favorable for computer programming.

In a non-ergodic case, the presented procedure can not

be directly adopted. This is because our proposed renormalization approach is rooted in the relations among the time evolution operators defined by Eqs. (8-10), the exponential decay of diffusion modes in the moment space, and the evolution paths in the path space, which implicitly depends on the assumption of the ergodicity of system states. In the non-ergodic case where a set of states can never evolve to or be transformed from another set of states (i.e., the network connectivity is absent), path integrals between these state sets are ill-posed and the diffusion over the network can be subdivided into several irrelevant sub-processes (i.e., the diffusion processes defined on two disconnected clusters are independent from each other). Dealing with these properties is crucial for our work since the SRG is oriented toward analyzing high-order interactions, which are usually sparsely distributed and may lack ergodicity.

Here we develop a divide-and-conquer approach. Our idea arises from the fact that we can treat the diffusion from one cluster (i.e., a connected component) to another cluster on any order as being decelerated to a condition with zero velocity (i.e., being infinitely slow). This infinitely long-term diffusion process contains no short-range high-order interactions and, therefore, should not be integrated out during renormalization. Consequently, the SRG does not need to deal with the diffusion across any pair of clusters and can focus on the diffusion within each cluster severally. In the k -iteration, we consider the following two cases:

- (A) If $\mathbf{G}_k^{(q)}$ is connected (i.e., the ergodicity holds), we directly apply steps (1-6) on $\mathbf{G}_k^{(q)}$ to guide the renormalization of p -order interactions and derive the inputs of the $(k+1)$ -iteration.
- (B) If $\mathbf{G}_k^{(q)}$ is disconnected (i.e., the ergodicity does not hold) and has r clusters denoted by C_1, \dots, C_r , we respectively apply steps (1-6) on each cluster of $\mathbf{G}_k^{(q)}$ to guide the renormalization of p -order interactions formed among the units that belong to this cluster. Specifically, we treat each cluster C_i as a network and input it into steps (1-6) with $\mathbf{G}_k^{(p)}$. Please note that the above procedure does not affect $\mathbf{G}_k^{(p)}$ if the selected cluster C_i is trivial (i.e., contains only one unit). After dealing with all r clusters, the obtained results are used for the $(k+1)$ -iteration.

In Fig. 3(b), we conceptually illustrate our approach, which enables us to relax the constraint on system ergodicity while implementing the SRG.

B. Critical time scale

After developing the renormalization procedure, we attempt to present a detailed analysis of the time scale $\tau^{(q)}$ and its associated scaling relation.

In the ergodic case, the setting of $\tau^{(q)}$ in the SRG (as we have mentioned in step (2)) is finished in 1-st iteration and required to make the specific heat, an indicator of the transitions of diffusion processes, maximize (see similar ideas in Ref. [10]). Specifically, we consider the q -order spectral entropy in the 1-st iteration of the SRG (see Ref. [42] for the definition of spectral entropy)

$$S_1^{(q)}(\tau^{(q)}) = -\text{tr} \left[\rho_1^{(q)} \log \left(\rho_1^{(q)} \right) \right], \quad (20)$$

$$= \log \left(\sum_{\lambda_1^{(q)}} \exp \left(-\tau^{(q)} \lambda_1^{(q)} \right) \right) + \tau^{(q)} \langle \lambda_1^{(q)} \rangle_{\rho}, \quad (21)$$

where $\langle \lambda_1^{(q)} \rangle_{\rho} = \text{tr} \left(\mathbf{L}_1^{(q)} \rho_1^{(q)} \right)$. The q -order specific heat is defined according to the first derivative of the q -order spectral entropy

$$X_1^{(q)}(\tau^{(q)}) = -\frac{d}{d \log(\tau^{(q)})} S_1^{(q)}(\tau^{(q)}), \quad (22)$$

$$= -\left(\tau^{(q)} \right)^2 \frac{d}{d \tau^{(q)}} \langle \lambda_1^{(q)} \rangle_{\rho}. \quad (23)$$

Please see Appendix A for detailed derivations. The value of $\tau^{(q)}$ is selected to ensure $\frac{d}{d \tau^{(q)}} X_1^{(q)}(\tau^{(q)}) = 0$, which indicates an infinite deceleration condition of diffusion processes. See Fig. 3(c) for illustrations. Apart from the infinite deceleration condition, determining the time scale value $\tilde{\tau}^{(q)}$ used in the step (2) of the SRG also requires us to consider the high-order properties of diffusion. For convenience, we denote $\tilde{\tau}^{(q)}$ as the value of $\tau^{(q)}$ under the infinite deceleration condition (i.e., there is $\frac{d}{d \tau^{(q)}} X_1^{(q)}(\tau^{(q)})|_{\tilde{\tau}^{(q)}} = 0$). The optimal time scale for the SRG is set as

$$\tilde{\tau}^{(q)} = \frac{2}{q+1} \tilde{\tau}^{(q)}, \quad (24)$$

which is the average subdivided time scale for each 1-simplex in a n -simplex (i.e., the average number of adjacent 1-simplexes between arbitrary units i and j is $\frac{n+1}{2}$). Note that $\tilde{\tau}^{(q)} = \tilde{\tau}^{(q)}$ holds for pairwise interactions.

The above procedure can be directly generalized to the non-ergodic case, where we treat each cluster C_i as a network and derive a $\tilde{\tau}^{(q)}$ for it if it has not been assigned with a time scale yet. The time scale of a cluster does not change after it is assigned. See Fig. 3(c) for illustrations.

After determining the time scale, the SRG proposed in Sec. IV A can be applied to renormalize interacting systems in a non-parametric manner. In Appendix B, we use the SRG to process a system whose pairwise interactions exhibit small-world properties [63] and illustrate how the renormalization flow changes across different combinations of (p, q) . This result qualitatively

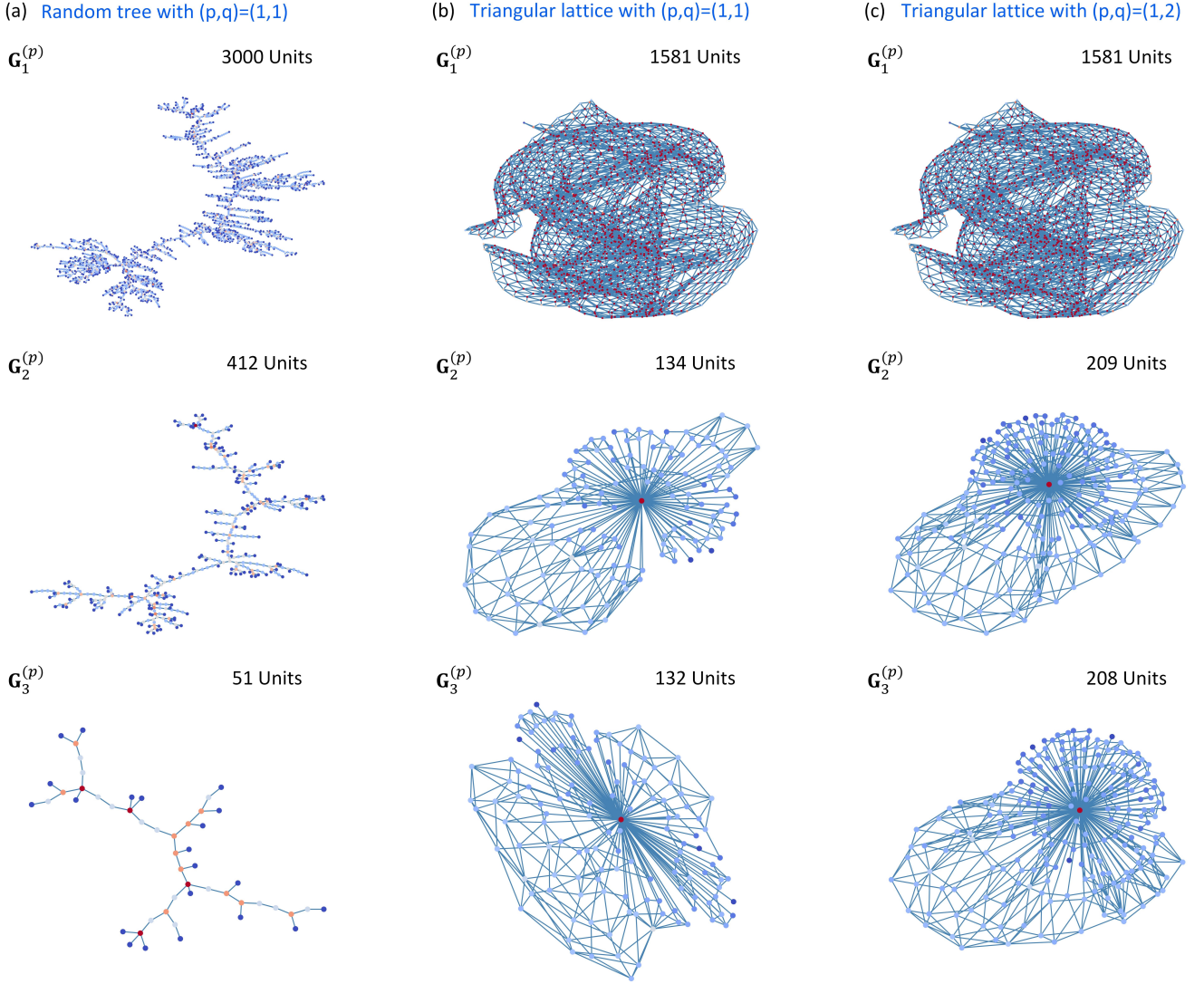


FIG. 4. Instances of the renormalization flows of the simplex renormalization group (SRG). The first three iterations of renormalization on the systems whose pairwise interactions follow the random tree (a) and the triangular lattice (b-c) are presented, where we set $(p, q) = (1, 1)$ and $(p, q) = (1, 2)$ for (a-b) and (c), respectively.

suggests the effects of higher-order interactions on lower-order interactions during renormalization, whose quantification is explored in our subsequent analysis. In Fig. 4, we present more instances of the SRG applied on synthetic interacting systems whose pairwise interactions follow scale-invariant structures (e.g., the random tree and the triangular lattice).

C. Scaling relation and high-order effects

Given the SRG, a crucial task is to analyze the potential scaling relation and quantify the effects of high-order interactions on it.

In the ergodic case, we denote $\tilde{X}^{(q)}$ and $\tilde{\rho}^{(q)}$ as the specific heat and density operator associated with $\tilde{\tau}^{(q)}$. We can insert these variables into Eq. (23) to derive the

following relation

$$\frac{\tilde{X}^{(q)}}{\tilde{\tau}^{(q)}} = \langle \lambda_1^{(q)} \rangle_{\tilde{\rho}} + \mu, \quad \forall \mu \in \mathbb{R}, \quad (25)$$

where $\langle \lambda_1^{(q)} \rangle_{\tilde{\rho}} = \text{tr}(\mathbf{L}_1^{(q)} \tilde{\rho}^{(q)})$ and constant μ is obtained when we solve Eq. (23) as a differential equation. If the Laplacian eigenvalue spectrum (i.e., the density of the eigenvalues of $\mathbf{L}_1^{(q)}$) follows a general power-law form $\text{Prob}(\lambda_1^{(q)}) \sim (\lambda_1^{(q)})^{\beta^{(q)}}$, we can obtain a scaling relation

$$\beta^{(q)} = \tilde{X}^{(q)} - 1 - \nu, \quad \exists \nu \in [0, \infty), \quad (26)$$

whose derivations are presented in Appendix C. Parameter ν is a specific constant. For a system with scale-invariance property on the q -order, the power-law form of

the Laplacian eigenvalue spectrum holds and should be invariant under the transformation of the SRG. Therefore, we expect to see an approximately constant $\tilde{X}^{(q)}$ in a certain interval of time scale (i.e., the infinite deceleration condition), accompanied by a fixed $\beta^{(q)}$ during renormalization. For a system without scale-invariance, the scaling relation vanishes.

To generalize our analysis to the non-ergodic case, we respectively derive $\tilde{\tau}^{(q)}(i)$ and $\beta^{(q)}(i)$ for each cluster C_i of $\mathbf{G}_k^{(q)}$ following Eqs. (25-26). These definitions enable us to obtain

$$\langle \lambda_k^{(q)} \rangle_{\tilde{\rho}} = \left\langle \frac{\beta^{(q)}(i) + 1}{\tilde{\tau}^{(q)}(i)} \right\rangle_i + \nu, \quad \exists \nu \in [0, \infty), \quad (27)$$

and

$$\tilde{X}^{(q)} = \tilde{\tau}^{(q)} \left\langle \frac{\beta^{(q)}(i) + 1}{\tilde{\tau}^{(q)}(i)} \right\rangle_i + \nu, \quad \exists \nu \in [0, \infty), \quad (28)$$

where $\langle \cdot \rangle_i$ denotes weighted averaging across all clusters of $\mathbf{G}_k^{(q)}$ (i.e., weighted according to cluster size). In the non-ergodic case, variables $\tilde{X}^{(q)}$ and $\tilde{\tau}^{(q)}$ refer to the global specific heat and the time scale measured on $\mathbf{L}_k^{(q)}$ under the infinite deceleration condition. Eqs. (25-26) actually serve as a special case of Eqs. (27-28) where there exists only one cluster. Please see Appendix D for derivations.

Eqs. (25-28) are derived for q -order interactions during renormalization and may divide from the original scaling relation of p -order interactions. These p -order interactions, initially corresponding to $\tilde{X}^{(p)}$ and $\beta^{(p)}$, are renormalized according to $\tilde{X}^{(q)}$ and $\beta^{(q)}$ in the SRG. In the case with $p < q$, we can measure the effects of q -order interactions on the scaling relation of p -order ones as

$$\zeta(p, q) = |\tilde{X}^{(p)} - \tilde{X}^{(q)}|, \quad (29)$$

which is applicable to both ergodic and non-ergodic cases.

Overall, the proposed SRG offers an opportunity to verify the potential existence of scale-invariance on different orders and classify interacting systems according to their high-order scaling properties.

V. APPLICATION OF THE SIMPLEX RENORMALIZATION GROUP

To this point, we have elaborated the SRG framework and its properties. Below, we validate its applicability in analyzing the systems with high-order interactions.

A. Verification of the multi-order scale-invariance

We aim at verifying the multi-order scale-invariance (i.e., being invariant under the SRG transformation on different orders). Specifically, being scale-invariant on an

order requires the system to be located at a non-trivial fixed point of the renormalization flow while a trivial Gaussian fixed point suggests a non-critical and weakly correlated system driven by the central limit theorem. In Appendix E, we implement our verification according to the behaviours of the Laplacian eigenvalue spectrum. Based on the existence of invariant power-law forms of Laplacian eigenvalue spectra under the SRG transformation, we can classify systems into scale-invariant, weak-scale-invariant, and scale-dependent types on different orders.

Apart from the above approach, there exists a more direct way to realize the verification. Because a scale-invariant system on q -order should invariably follow the scaling relation, being born to satisfy Eq. (27) is one of the necessary conditions of being scale-invariant. Consequently, we can first measure the deviations from the scaling relation of concerned systems before renormalization. Given significantly large deviations, the system can not be scale-invariant no matter how it behaves during renormalization. In Fig. 5, the measurement is conducted on multiple types of systems when $k = 1$ (see Appendix F for details). As shown in Figs. 5(a-e), although the mean observations of $(\tilde{X}^{(q)}, \tilde{\tau}^{(q)} \left\langle \frac{\beta^{(q)}(i) + 1}{\tilde{\tau}^{(q)}(i)} \right\rangle_i + \nu)$ averaged across all replicas collapse onto the scaling relation on every order, the departures from the scaling relation measured by the standard deviations of $\tilde{X}^{(q)}$ and $\tilde{\tau}^{(q)} \left\langle \frac{\beta^{(q)}(i) + 1}{\tilde{\tau}^{(q)}(i)} \right\rangle_i + \nu$ in some systems can be non-negligible. Specifically, as suggested in Fig. 5(f), the systems whose pairwise interactions follow known scale-invariant structures, such as the triangular lattice or the random tree, do ensure that all their replicas follow the scaling relation with vanishing deviations. The replicas of the systems whose pairwise interactions follow the Barabási-Albert network, a structure with weak scale-invariant property (i.e., the Barabási-Albert network can be renormalized within a specific set of scales but is not strictly scale-invariant [10]), have relatively small deviations on the first three orders as well. The replicas of other kinds of systems whose pairwise interactions follow the Watts-Strogatz or the Erdos-Renyi networks [64] exhibit larger deviations from the scaling relation, suggesting the absence of scale-invariance.

In sum, the method reported in Fig. 5 can offer a convenient detection of scale-dependent systems in practice. Note that this method alone is not sufficient to confirm scale-invariant systems because satisfying Eq. (27) before renormalization only serves as a necessary condition of scale-invariance. To seek a more comprehensive verification, one should apply the approach in Appendix E or repeat the analysis in Fig. 5 on every k -th iteration of renormalization (i.e., to verify whether the scaling relation is invariably followed).

Finally, we measure the high-order effects on the scaling relation applying Eq. (29). As shown in Figs. 5(g-i), these high-order effects are non-negligible and generally increase with the difference between p and q . These

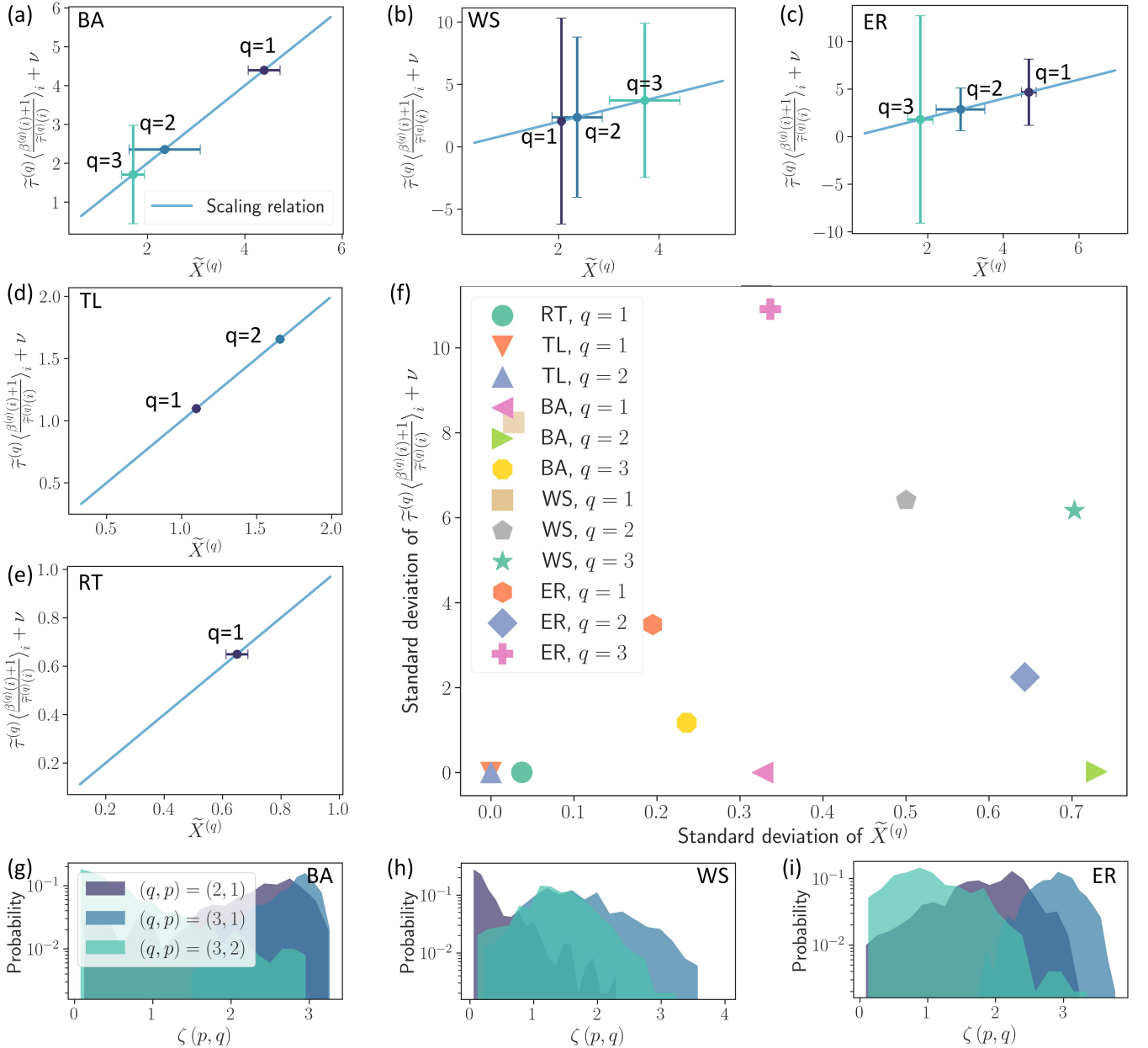


FIG. 5. Scaling relation of the simplex renormalization group. (a-e) We verify the scaling relation on the systems whose pairwise interactions follow a Barabási-Albert network (BA, $c = 10$), a Watts-Strogatz network (WS, each unit initially has 10 neighbors and edges are rewired according to a probability of 0.1), and an Erdos-Renyi network (ER, two units share an edge with a probability of 0.2), the triangular lattice (TL, with the interactions of the first two orders), and the random tree (RT, with only pairwise interactions), respectively. Scatters denote the mean values of $\left(\tilde{X}^{(q)}, \tilde{\tau}^{(q)} \left\langle \frac{\beta^{(q)}(i)+1}{\tilde{\tau}^{(q)}(i)} \right\rangle_i + \nu \right)$ averaged across all replicas on each order and error bars denote standard deviations. (f) The standard deviations compared across different systems. (g-i) The high-order effects measured on the replicas in (a-c).

results explain how the SRG differs from conventional renormalization groups that focus on a single order.

B. Identification of organizational structure

Then, we turn to validate the applicability of the SRG in identifying organizational structures (e.g., latent communities) of complex systems.

If organizational structures are given, we explore the conditions under which these structures can be main-

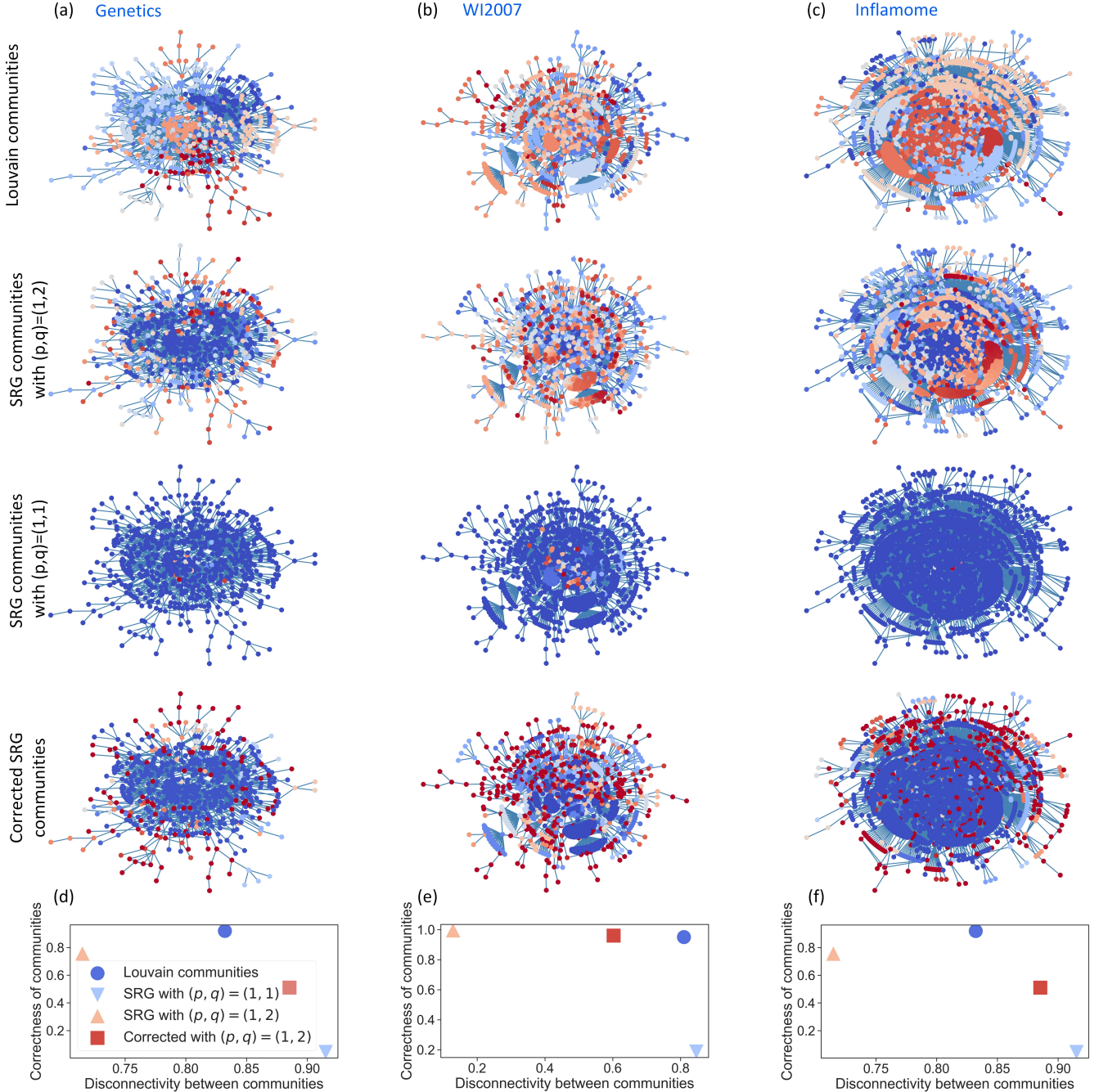


FIG. 6. The organizational structure discovered by renormalization flows. (a-c) The Louvain communities underlying the Genetics, WI2007, and Inflamome data sets [65] are extracted using the Louvain community detection algorithm [66]. The units of different communities are distinguished by colors. For comparison, the SRG is applied to renormalize these systems with $(p, q) = (1, 2)$ and $(p, q) = (1, 1)$. Units are determined as belonging to the same SRG community if they are aggregated into the same super-unit. Meanwhile, the corrected SRG communities are presented. (d-f) The correctness of communities and disconnectivity between communities are shown.

tained by the SRG. In Appendix G, we implement the verification using protein-protein interactions (e.g., orthologous and genetic interactions) in *Caenorhabditis elegans* [65]. We first extract the initial community structures of protein-protein interactions by applying the Louvain community detection algorithm [66]. Then, we use

the SRG to renormalize protein-protein interactions on a high order (i.e., with $(p, q) = (1, 2)$) or a low order (i.e., with $(p, q) = (1, 1)$). We define latent community structures according to unit aggregation during renormalization (see Appendix G for details). Consistent with Ref. [38], our results in Appendix G highlight that renormal-

ization can never be treated as a trivial counterpart of clustering. Meanwhile, the SRG guided by high-order interactions (e.g., $q = 2$) can generally preserve the properties of initial community structures while the SRG guided by pairwise interactions does not. Based on these results, we speculate that high-order interactions are essential in forming and characterizing organizational structures. Communities can not be treated as the trivial collections of pairwise interactions.

If organizational structures are not given, we explore whether the SRG can be applied to identify latent community structures. In Fig. 6, we define communities according to the renormalization flows of the SRG and compare them with the Louvain communities. Specifically, we classify the units into the same SRG community if they are aggregated into the same super-unit during renormalization (e.g., we generate SRG communities after the first iteration of renormalization flows in Fig. 6). To quantitatively compare the SRG communities with the Louvain communities, we analyze the correctness of communities (i.e., or referred to as the performance) [67] and the disconnectivity between communities (i.e., or referred to as the coverage) [67]. Note that both these concepts reflect the properties of communities on 1-order because they are defined on pairwise interactions [67]. As shown in Fig. 6, the behaviours of SRG are different from the Louvain community detection algorithm, which is designed to maximize the modularity of communities [66, 68, 69]. When the SRG is guided by pairwise interactions, the generated SRG communities tend to be disconnected with each other (i.e., lack pairwise interactions across communities) and have low accuracy (i.e., units in the same community may lack pairwise interactions because lots of short-range pairwise interactions are reduced). When the SRG is guided by high-order interactions, the generated SRG communities tend to be precise (i.e., units in the same community always involve in high-order interactions) and non-isolated (i.e., there exist across-community pairwise interactions since the SRG mainly reduces high-order interactions). We are inspired to generate the SRG communities by combining the properties of these two cases. We suggest considering pairwise interactions to correct the SRG communities generated by the SRG guided by high-order interactions. Specifically, for two SRG communities generated with $(p, q) = (1, 2)$, if at least half of the units in one community have pairwise interactions with the units in another community, then all units in these two SRG communities are merged into the same community. The corrected SRG communities are presented in Fig. 6, exhibiting better capability in balancing between the correctness and the disconnectivity.

Taken together, although the SRG does not behave in a manner similar to the community detection algorithm, it does offer a way to identify possible latent organizational structures. The properties of the SRG communities vary across different orders. After considering multiple orders, the corrected SRG communities have the potential to of-

fer a system partition scheme competitive to optimized algorithms.

C. Optimization of information bottleneck

Finally, we analyze the SRG in terms of informational properties. In previous studies, the analysis using information theory has suggested that renormalization groups essentially maximize the mutual information between relevant features and the environment [70, 71] or reduce the mutual information among irrelevant features [72]. In this work, we suggest exploring the SRG from the perspective of information bottleneck [73] because renormalization groups, similar to dimensionality reduction or representation learning approaches in machine learning [74–76], essentially deal with information encoding during data compression [77].

To realize this analysis, we follow one of our earlier works [78] to represent the associated high-order network sketch in the k -th iteration of the renormalization flow, $\mathbf{G}_k^{(p)}$, by a Gaussian variable

$$\mathbf{X}_k^{(p)} \sim \mathcal{N} \left(\mathbf{0}, \mathbf{L}_k^{(p)} + \frac{1}{N_k^{(p)}} \mathbf{J} \right), \quad (30)$$

where \mathbf{J} is an all-one matrix and $N_k^{(p)}$ measures the number of units in $\mathbf{G}_k^{(p)}$. The derived Gaussian variable offers a optimal representation of $\mathbf{G}_k^{(p)}$ with network-topology-dependent smoothness and maximum entropy properties and enable us to compare $\mathbf{G}_k^{(p)}$ across different iterations (see Ref. [78] for explanations). If necessary, one can further add a scaled unitary matrix, $a\mathbf{I}$ ($a > 0$), to the covariance matrix of $\mathbf{X}_k^{(p)}$ to ensure its semi-positive property in the non-ergodic case (i.e., the case where $\mathbf{G}_k^{(p)}$ is disconnected).

We suggest to consider the following information bottleneck

$$\mathcal{L}_{IB} = \underbrace{\mathcal{I} \left(\mathbf{X}_k^{(p)} ; \mathbf{X}_1^{(p)} \right)}_{\text{Preserved information}} - \psi \underbrace{\mathcal{I} \left(\mathbf{X}_k^{(p)} ; \mathbf{X}_i^{(p)} \right)}_{\text{Complexity}}, \quad \forall \psi > 0 \quad (31)$$

where $i = k - 1$ if $k > 1$ and $i = k$ if $k = 1$. Parameter ψ denotes the regularization strength. Notion $\mathcal{I}(\cdot; \cdot)$ denotes the mutual information, which can be estimated by the mutual information estimator with local non-uniformity corrections [79] (we set the correction strength as 10^{-3} such that corrections only happen when necessary). This approach has been included in the non-parametric entropy estimation toolbox [80]. Note that Eq. (31) is different from the information bottleneck considered in Ref. [77] due to the discrepancy between our concerned question and Ref. [77].

Intuitively, the objective function in Eq. (31) evaluates whether the renormalized system in the k -th iteration,

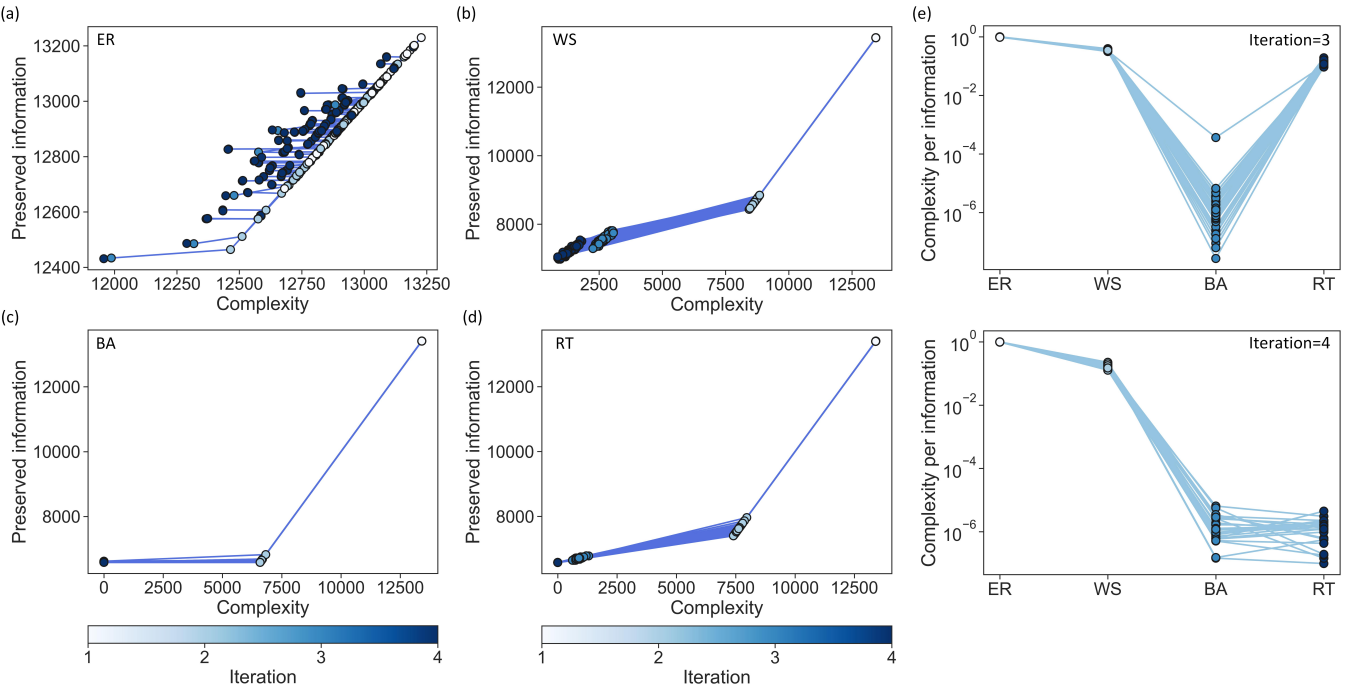


FIG. 7. The information curve of the SRG. (a-d) The SRG is applied on four synthetic interacting systems, whose pairwise interactions follow the Erdos-Renyi network (ER, each pair of units share an edge with a probability of 0.01), the Watts-Strogatz network (WS, each unit initially has 5 neighbors and edges are rewired according to a probability of 0.05), the Barabási-Albert network (BA, $c = 1$), and the random tree (RT), respectively. Each kind of system consists of 500 units and has 100 replicas. The SRG is defined with the multi-order Laplacian and $(p, q) = (1, 1)$ for RT while $(p, q) = (1, 2)$ is set for all other systems. The generated information flows are used to derive information curves. (e) The complexity per preserved information bit is shown.

$\mathbf{G}_k^{(p)}$, preserves the information of the original system, $\mathbf{G}_1^{(p)}$, by maximizing $\mathcal{I}(\mathbf{X}_k^{(p)}; \mathbf{X}_1^{(p)})$ and reduces the trivial dependence on its previous state, $\mathbf{G}_i^{(p)}$, by minimizing $\mathcal{I}(\mathbf{X}_k^{(p)}; \mathbf{X}_i^{(p)})$. For a valid renormalization group, being able to preserve some information of the original system is an essential capability. Because a trivial solution of maximizing $\mathcal{I}(\mathbf{X}_k^{(p)}; \mathbf{X}_1^{(p)})$ is to make $\mathbf{G}_k^{(p)} = \mathbf{G}_{k-1}^{(p)}$ for any $k > 1$ (i.e., there is no renormalization at all), we need to include the complexity term in Eq. (31) to avoid this trivial result.

Meanwhile, the possibility of maximizing $\mathcal{I}(\mathbf{X}_k^{(p)}; \mathbf{X}_1^{(p)})$ depends on the properties of the system as well. If the system is scale-invariant, the preserved information does not rapidly vanish when we reduce the complexity since the information of $\mathbf{G}_1^{(p)}$ holds across scales (note that $\mathcal{I}(\mathbf{X}_k^{(p)}; \mathbf{X}_1^{(p)})$ still reduces slightly because the decreasing dimensionality of $\mathbf{X}_k^{(p)}$ affects the numerical behaviours of the estimator). If the system is scale-dependent, the preserved information crucially relies on the complexity and vanishes unless the complexity is high. Therefore, we can divide $\mathcal{I}(\mathbf{X}_k^{(p)}; \mathbf{X}_1^{(p)})$ by $\mathcal{I}(\mathbf{X}_k^{(p)}; \mathbf{X}_i^{(p)})$ to measure the complexity required

by a single bit of preserved information in the k -th iteration. A high value of complexity per information bit suggests that the system is scale-dependent because we can not find a low-complexity coarse-grained system to represent it efficiently.

In Figs. 7(a-d), we show the information curves of the renormalization flows generated on four kinds of interacting systems. As suggested by our results, the renormalization flows of weak-scale-invariant (e.g., BA) and scale-invariant (e.g., RT) systems lead to sufficiently small complexity values and numerous preserved information bits while the renormalization flows of scale-dependent systems (e.g., ER and WS) do not. The information bits of scale-dependent systems are preserved at the cost of maintaining high complexity. These results can be quantitatively validated based on the complexity per information bit measured in Fig. 7(e). These findings suggest the possibility of verifying scale-invariance from an informational perspective.

VI. DISCUSSIONS

Various real interacting systems share universal characteristics that govern their dynamics and phase transition behaviours [81]. These characteristics remain elusive because fundamental physics tools, such as path

integrals and renormalization group theories, are not well-established when *a priori* knowledge about system mechanisms is absent [10]. This gap may be accountable for diverse controversies concerning the critical phenomena in biological or social systems (e.g., the controversies about brain criticality [82]) and has induced a booming field that is devoted to developing statistical physics approaches for the empirical data generated by unknown mechanisms [10]. Notable progress is accomplished in the computational implementations of path integrals and renormalization groups on real systems with pairwise interactions [10, 29–33], supporting remarkable applications in analyzing neural dynamics [83] and swarm behaviours [84]. Nevertheless, there exists no apparent equivalence between these pioneering works and an appropriate approach for analyzing un-decomposable high-order interactions because classic network or geometric representations are invalid in characterizing polyadic relations [9, 11–14].

In this work, we contribute to the field by developing the natural generalizations of path integrals and renormalization groups on un-decomposable high-order interactions. Our main contributions are summarized below:

- (1) Our theoretical derivations lead us to an intriguing perspective that the system evolution governed by high-order interactions can be fully formalized by path integrals on simplicial complexes (e.g., the return probability of an arbitrary system state is proportional to the path integral of all closed curves that start from and end with this state in high-order networks), which suggests the possibility for studying high-order interactions applying the tools of quantum field theory [3, 4].
- (2) We suggest that the contributions of microscopic fluctuations to macroscopic states in the moment space are precisely characterized by a function of the multi-order Laplacian [9] or our proposed high-order path Laplacian. Consequently, a renormalization group, the SRG, can be directly developed based on the diffusion on simplicial complexes, which does not require any assumption on latent metric for mapping units into target spaces (e.g., the hyperbolic space [30, 33]). This property ensures the general applicability of our theory on real complex systems, where *a priori* knowledge is rare and any assumption can be unreliable. Different from classic renormalization groups, the SRG can renormalize p -order interactions in a system based on the structure and dynamics associated with q -order interactions ($p \leq q$), enabling us to analyze the effects of q -order interactions on p -order ones and study the scaling properties across different orders.
- (3) We propose a divide-and-conquer approach to deal with non-ergodic cases, where some system states are never reachable by the evolution started from

other systems states (i.e., without global connectivity). The developed framework improves the validity of our theory for high-order interactions, which usually feature sparse distributions that break system ergodicity on a high order.

- (4) We seek for a comprehensive analysis of the scaling relation in both ergodic and non-ergodic cases. Our theoretical derivations and computational experiments suggest that the scaling relation can help differentiate among scale-invariant, weak-scale-invariant, and scale-dependent systems on an arbitrary order (consistent with verification using the behaviours of the Laplacian eigenvalue spectrum). Meanwhile, the effects of high-order interactions on the scaling relation can be measured as well.
- (5) Apart from validating the essential difference between the SRG and clustering [38], our experiments also suggest the applicability of the SRG in identifying organizational structures (e.g., latent communities) of real complex systems and analyzing the crucial roles of the interactions of different orders in characterizing these structures.
- (6) We suggest that the SRG can be analyzed from the perspective of information bottleneck, which quantifies how the renormalized system preserves the information of its original properties while reducing complexity. We discover that the complexity required for maintaining one information bit can distinguish between scale-invariant and scale-dependent systems in an informational aspect.

In sum, by extending classic path integrals and renormalization groups to simplicial complexes, our research reveals a novel route to studying the universality classes of complex systems with intertwined high-order interactions. The proposed simplex path integral and simplex renormalization group can serve as precise tools for characterizing system dynamics, discovering intrinsic scales, and verifying potential scale invariance on different orders. The revealed information by our theory may shed light on the intricate effects of the interplay among multi-order interactions on system dynamics properties (e.g., phase transitions or scale invariance). To ensure the capacity of our theory in analyzing the real data sets that are governed by unknown mechanisms or lack clear network structures, we suggest to consider *a-priori*-knowledge-free framework in future studies. This framework begins with applying specific non-negative non-parametric metrics (e.g., distance correlation [85] or co-mutual information [86]) to evaluate the coherence between units and define the adjacency matrix of pairwise interactions. Then, the high-order representation and the simplex renormalization group can be progressively calculated following our theory.

ACKNOWLEDGEMENTS

This project is supported by the Artificial and General Intelligence Research Program of Guo Qiang Research

Institute at Tsinghua University (2020GQG1017) as well as the Tsinghua University Initiative Scientific Research Program. Authors appreciate Hedong Hou, who studies at the Institut de Mathématiques d'Orsay, for his inspiring discussions.

Appendix A: The behaviour of the specific heat

Here we present the derivations of the specific heat in Eq. (23), $X_1^{(q)}(\tau^{(q)})$ when $\tau^{(q)}$ is sufficiently large. Formally, Eq. (22) is solved as

$$X_1^{(q)}(\tau^{(q)}) = -\tau^{(q)}\langle\lambda_1^{(q)}\rangle_\rho - \left(\tau^{(q)}\right)^2 \frac{d}{d\tau^{(q)}}\langle\lambda_1^{(q)}\rangle_\rho - \tau^{(q)} \frac{d}{d\tau^{(q)}} \log \left(\sum_{\lambda_1^{(q)}} \exp(-\tau^{(q)}\lambda_1^{(q)}) \right), \quad (A1)$$

where the third term can be reformulated as

$$-\tau^{(q)} \frac{d}{d\tau^{(q)}} \log \left(\sum_{\lambda_1^{(q)}} \exp(-\tau^{(q)}\lambda_1^{(q)}) \right) = -\tau^{(q)} \frac{1}{\sum_{\lambda_1^{(q)}} \exp(-\tau^{(q)}\lambda_1^{(q)})} \frac{d}{d\tau^{(q)}} \sum_{\lambda_1^{(q)}} \exp(-\tau^{(q)}\lambda_1^{(q)}), \quad (A2)$$

$$= \tau^{(q)} \frac{\sum_{\lambda_1^{(q)}} \lambda_1^{(q)} \exp(-\tau^{(q)}\lambda_1^{(q)})}{\sum_{\lambda_1^{(q)}} \exp(-\tau^{(q)}\lambda_1^{(q)})}, \quad (A3)$$

$$= \tau^{(q)} \langle \lambda_1^{(q)} \rangle_\rho. \quad (A4)$$

Inserting Eq. (A4) into Eq. (A1), we can readily derive

$$X_1^{(q)}(\tau^{(q)}) = -\left(\tau^{(q)}\right)^2 \frac{d}{d\tau^{(q)}} \langle \lambda_1^{(q)} \rangle_\rho. \quad (A5)$$

Appendix B: Comparison of the SRG across different settings of (p, q)

In Fig. 8, we use the SRG to process a system whose pairwise interactions exhibit small-world properties [63].

We first renormalize the system on the p -order under the guidance of q -order interactions ($p = 1$ and $q = 2$). As shown in Fig. 8(a), integrating out short-range q -order interactions lead to an organizational-structure-preserving renormalization flow of p -order interactions. Because high-order interactions are usually distributed in a sparser manner than pairwise ones (e.g., see the flow of $\mathbf{G}^{(q)}$), the renormalization flow guided by q -order interactions reduce the system less drastically.

For comparison, we renormalize the system on the p -order according to the properties of p -order interactions themselves (i.e., this is equivalent to setting $p = q = 1$ in the SRG) in Fig. 8(b). The generated renormalization flow reduces the system more significantly because p -order interactions, including those short-range ones, are distributed in a dense manner. The differences between Fig. 8(a) and Fig. 8(b) qualitatively suggest the effects of higher-order interactions on lower-order interactions during renormalization.

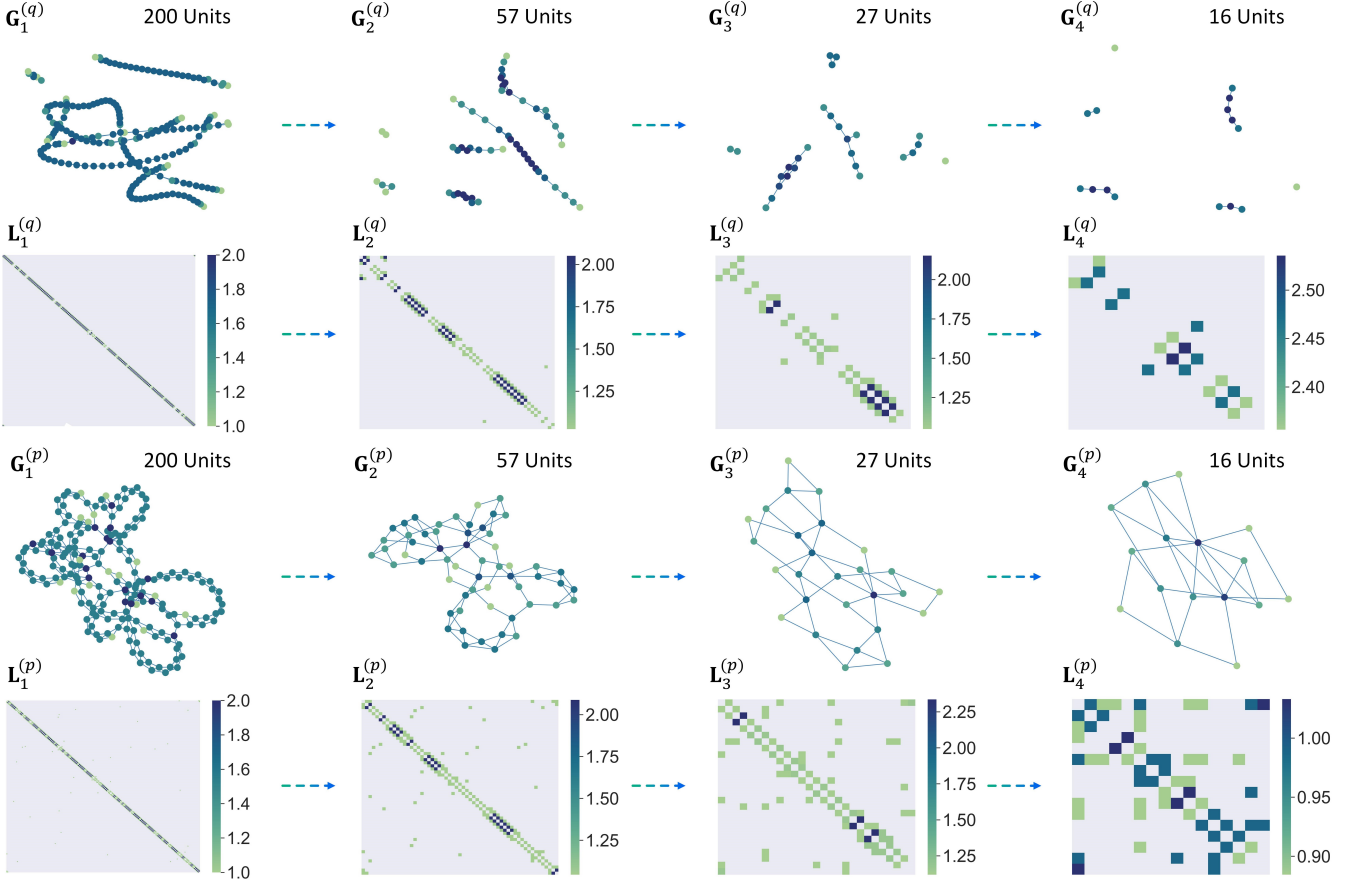
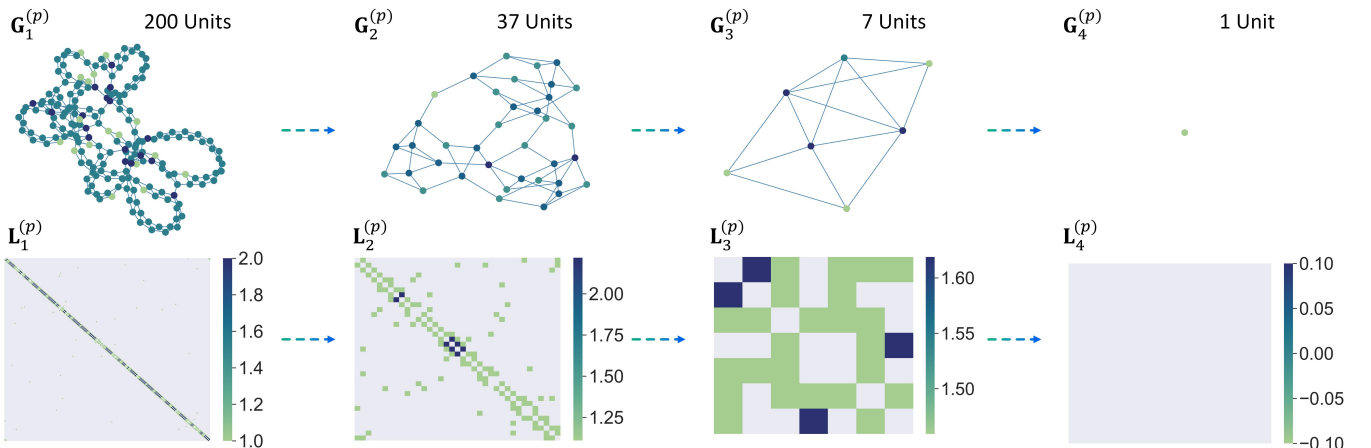
(a) The case with $p=1$ and $q=2$ (b) The case with $p=1$ and $q=1$ 

FIG. 8. The simplex renormalization group (SRG) with different (p, q) . (a) We generate a system with 200 units whose pairwise interactions follow a Watts-Strogatz network (each unit initially has 5 neighbors and edges are rewired according to a probability of 0.05) [63]. Then, the SRG is applied to renormalize the system on the p -order according to the properties of q -order interactions ($p = 1$ and $q = 2$). The first five iterations of the renormalization flows on q - and p -orders are presented, accompanied by their corresponding high-order path Laplacian operators. (b) For comparison, we show the renormalization flow of the system on the p -order guided by the q -order when $p = q = 1$.

Appendix C: Scaling relation of the Laplacian eigenvalue spectrum in the ergodic case

Given the general form of the Laplacian eigenvalue spectrum, i.e., $\text{Prob} \left(\lambda_1^{(q)} \right) \sim \left(\lambda_1^{(q)} \right)^{\beta^{(q)}} = \alpha \left(\lambda_1^{(q)} \right)^{\beta^{(q)}}$, we can first reformulate Eq. (25) in the main text as

$$\frac{\tilde{X}^{(q)}}{\tilde{\tau}^{(q)}} = \langle \lambda_1^{(q)} \rangle_{\tilde{\rho}} + \mu, \quad (\text{C1})$$

$$= \frac{\frac{1}{N_k^{(q)}} \sum_{\lambda_1^{(q)}} \lambda_1^{(q)} \exp \left(-\tilde{\tau}^{(q)} \lambda_1^{(q)} \right)}{\frac{1}{N_k^{(q)}} \sum_{\lambda_1^{(q)}} \exp \left(-\tilde{\tau}^{(q)} \lambda_1^{(q)} \right)} + \mu, \quad (\text{C2})$$

$$= \frac{\int_0^{\infty} \alpha \left(\lambda_1^{(q)} \right)^{\beta^{(q)}+1} \exp \left(-\tilde{\tau}^{(q)} \lambda_1^{(q)} \right) d\lambda_1^{(q)}}{\int_0^{\infty} \alpha \left(\lambda_1^{(q)} \right)^{\beta^{(q)}} \exp \left(-\tilde{\tau}^{(q)} \lambda_1^{(q)} \right) d\lambda_1^{(q)}} + \mu, \quad \exists \mu \in \mathbb{R}. \quad (\text{C3})$$

Using the Euler's gamma function, i.e., $\Gamma(z) = \int_0^{\infty} x^{z-1} \exp(-x) dx$, we can transform Eq. (C3) as

$$\frac{\tilde{X}^{(q)}}{\tilde{\tau}^{(q)}} = \frac{\frac{\alpha}{(\tilde{\tau}^{(q)})^{\beta^{(q)}+2}} \Gamma(\beta^{(q)}+2)}{\frac{\alpha}{(\tilde{\tau}^{(q)})^{\beta^{(q)}+1}} \Gamma(\beta^{(q)}+1)} + \mu, \quad (\text{C4})$$

which directly leads to

$$\tilde{X}^{(q)} = \frac{\Gamma(\beta^{(q)}+2)}{\Gamma(\beta^{(q)}+1)} + \mu \tilde{\tau}^{(q)}, \quad (\text{C5})$$

$$= \beta^{(q)} + 1 + \nu, \quad \exists \nu \in [0, \infty). \quad (\text{C6})$$

Note that we have reduce $\mu \tilde{\tau}^{(q)}$ in Eq. (C5) to ν in Eq. (C6) for convenience, where ν denotes an arbitrary non-negative number. The scope of $\nu \in [0, \infty)$ is derived from the fact that $\beta^{(q)} \leq -1$ (i.e., as required by the power-law distribution) and $\tilde{X}^{(q)} \geq 0$ (i.e., the specific heat is non-negative).

Appendix D: Scaling relation of the Laplacian eigenvalue spectrum in the non-ergodic case

Here we present the derivations of the scaling relation in the non-ergodic case. For convenience, we denote $\mathbf{L}_k^{(q)}(i)$ as the Laplacian of cluster C_i of $\mathbf{G}_k^{(q)}$. It is clear that the Laplacian of $\mathbf{G}_k^{(q)}$ can be formulated in a block diagonal form

$$\mathbf{L}_k^{(q)} = \text{diag} \left(\left[\mathbf{L}_k^{(q)}(1), \dots, \mathbf{L}_k^{(q)}(r) \right] \right) \quad (\text{D1})$$

because there exists no interaction between each pair of clusters. Eq. (D1) leads to an important property of the determinant

$$\det \left(\mathbf{L}_k^{(q)} \right) = \prod_{i=1}^r \det \left(\mathbf{L}_k^{(q)}(i) \right), \quad (\text{D2})$$

$$\prod_{\lambda_k^{(q)} \in \Lambda_k^{(q)}} \lambda_k^{(q)} = \prod_{i=1}^r \prod_{\lambda_k^{(q)} \in \Lambda_k^{(q)}(i)} \lambda_k^{(q)}, \quad (\text{D3})$$

where $\Lambda_k^{(q)}$ and $\Lambda_k^{(q)}(i)$ denote the eigenvalue sets of $\mathbf{L}_k^{(q)}$ and $\mathbf{L}_k^{(q)}(i)$, respectively. According to Eqs. (D2-D3), the characteristic polynomial roots of $\mathbf{L}_k^{(q)}$ can be constructed using the combination of the characteristic polynomial roots of $\{\mathbf{L}_k^{(q)}(1), \dots, \mathbf{L}_k^{(q)}(r)\}$

$$\Lambda_k^{(q)} = \bigcup_{i=1}^r \Lambda_k^{(q)}(i). \quad (\text{D4})$$

Because each eigenvalue set $\Lambda_k^{(q)}(i)$ follows an independent distribution $\text{Prob}_i\left(\lambda_k^{(q)}\right) \sim \left(\lambda_k^{(q)}\right)^{\beta^{(q)}(i)} = \alpha(i) \left(\lambda_k^{(q)}\right)^{\beta^{(q)}(i)}$, the eigenvalue set $\Lambda_k^{(q)}$ defined by the weighted mixture (i.e., weighted according to cluster size) of $\{\Lambda_k^{(q)}(1), \dots, \Lambda_k^{(q)}(r)\}$ in Eq. (D4) is expected to follow

$$\text{Prob}\left(\lambda_k^{(q)}\right) = \sum_{i=1}^r \frac{|\Lambda_k^{(q)}(i)|}{\sum_{j=1}^r |\Lambda_k^{(q)}(j)|} \text{Prob}_i\left(\lambda_k^{(q)}\right). \quad (\text{D5})$$

This property enable us to relate the expectation of $\Lambda_k^{(q)}$ with the expectations of $\{\Lambda_k^{(q)}(1), \dots, \Lambda_k^{(q)}(r)\}$

$$\langle \lambda_k^{(q)} \rangle_{\tilde{\rho}} = \sum_{i=1}^r \frac{|\Lambda_k^{(q)}(i)|}{\sum_{j=1}^r |\Lambda_k^{(q)}(j)|} \langle \lambda_k^{(q)} \rangle_{\tilde{\rho}(i)}, \quad (\text{D6})$$

where $\tilde{\rho}^{(q)}(i)$ is the density operator associated with $\mathbf{L}_k^{(q)}(i)$. Given that each eigenvalue set $\Lambda_k^{(q)}(i)$ satisfies

$$\langle \lambda_k^{(q)} \rangle_{\tilde{\rho}(i)} = \frac{\beta^{(q)}(i) + 1}{\tilde{\tau}^{(q)}(i)} + \nu, \quad \exists \nu \in [0, \infty) \quad (\text{D7})$$

according to Eqs. (25-26) in the main text, we can derive

$$\langle \lambda_k^{(q)} \rangle_{\tilde{\rho}} = \sum_{i=1}^r \frac{|\Lambda_k^{(q)}(i)|}{\sum_{j=1}^r |\Lambda_k^{(q)}(j)|} \frac{\beta^{(q)}(i) + 1}{\tilde{\tau}^{(q)}(i)} + \sum_{i=1}^r \frac{|\Lambda_k^{(q)}(i)|}{\sum_{j=1}^r |\Lambda_k^{(q)}(j)|} \nu, \quad (\text{D8})$$

$$= \left\langle \frac{\beta^{(q)}(i) + 1}{\tilde{\tau}^{(q)}(i)} \right\rangle_i + \nu, \quad (\text{D9})$$

where $\langle \cdot \rangle_i$ denotes the weighted average across all clusters. Note that we have reduced the second term of Eq. (D8) into ν given the arbitrariness of ν . Eq. (D9) further leads to

$$\tilde{X}^{(q)} = \tilde{\tau}^{(q)} \left\langle \frac{\beta^{(q)}(i) + 1}{\tilde{\tau}^{(q)}(i)} \right\rangle_i + \nu, \quad \exists \nu \in [0, \infty), \quad (\text{D10})$$

where $\tilde{X}^{(q)}$ is the global specific heat measured on $\mathbf{L}_k^{(q)}$ under the infinite deceleration condition and $\tilde{\tau}^{(q)}$ denotes the corresponding time scale.

Appendix E: Extended results of the multi-order scale-invariance

In this section, we present the extended results of multi-order scale-invariance verification. Our verification is implemented using the behaviours of the Laplacian eigenvalue spectrum.

We implement our experiments on multiple types of synthetic interacting systems, whose pairwise interactions follow the Barabási-Albert network (BA, $c = 1$ or $c = 10$), the Watts-Strogatz network (WS, each unit initially has 10 neighbors and edges are rewired according to a probability of 0.1), the Erdos-Renyi network (ER, each pair of units share an edge with a probability of 0.01), the triangular lattice (TL), and the random tree (RT), respectively. Each kind of system consists of 1000 units and has 1000 replicas.

As shown in Fig. 9, the interacting systems whose pairwise interactions follow weak-scale-invariant (e.g, BA) and scale-invariant (e.g, TL and RT) structures exhibit multi-order scale invariance because their Laplacian eigenvalue spectra generally follow fixed power-law distributions during renormalization (note that noises in Laplacian eigenvalue spectra are unavoidable due to the numerical instability of eigen-decomposition in sparse matrices). For comparisons, the absence of multi-order scale invariance can be observed in the interacting systems with scale-dependent pairwise interactions (e.g, ER and WS). These results are consistent with our findings in Fig. 5, where the degrees to which the scaling relation holds are higher in scale-invariant and weak-scale-invariant systems (i.e., with smaller deviations) and are lower in other systems. In fact, the departures from the scaling relation of scale-dependent systems arise from the absence of power-law behaviours (e.g., see Fig. 9(b-c)). Apart from the verification of multi-order scale invariance, the results shown in Fig. 9 also support the study of the effects of high-order interactions on power-law behaviours. When the SRG is guided by 2-order interactions, the Laplacian eigenvalue spectra of the interacting systems whose

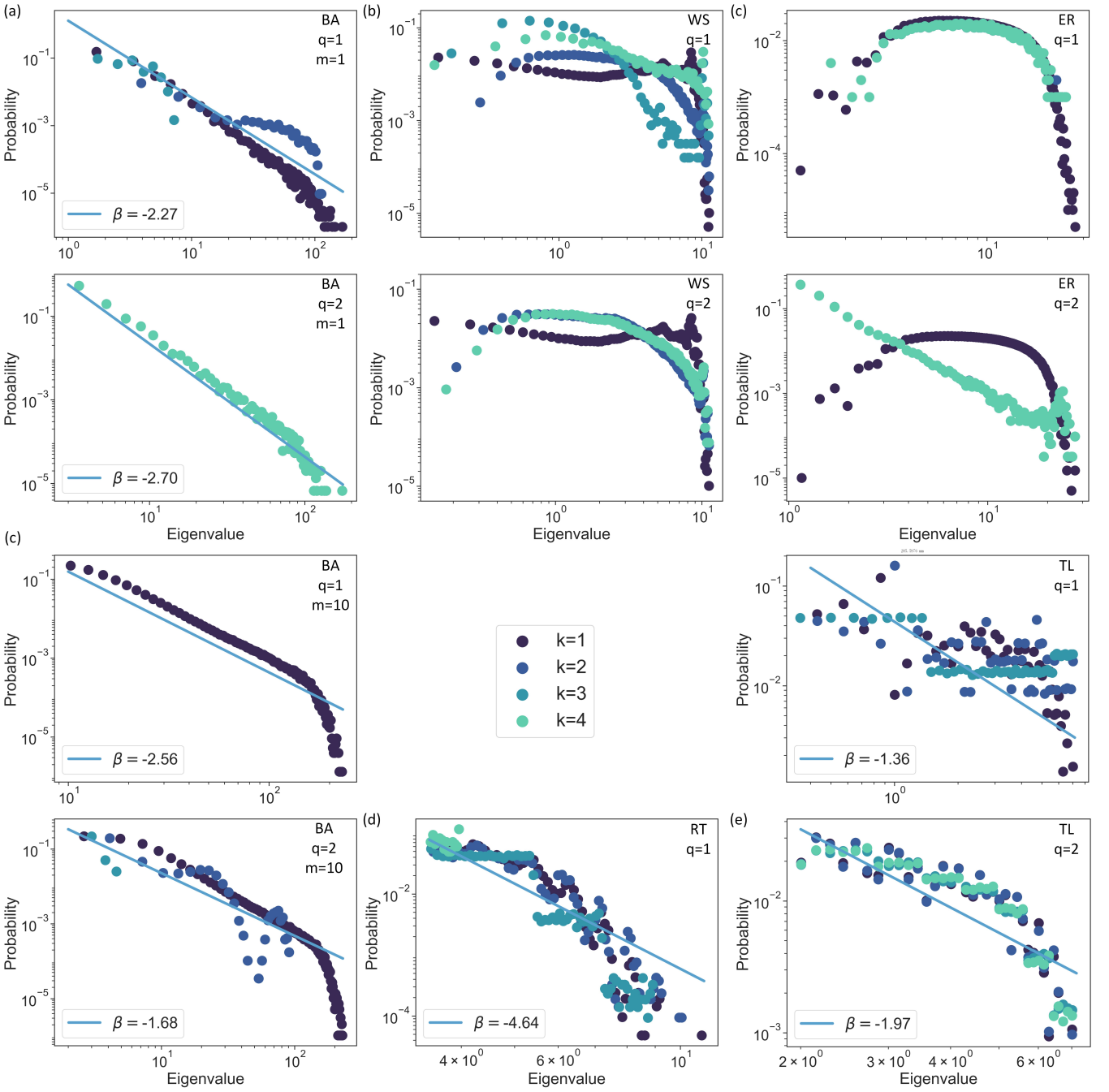


FIG. 9. The existence of the multi-order scale-invariance (Part I). (a-e) The degree distributions and the Laplacian eigenvalue spectra of different synthetic interacting systems under the transformation of the SRG are illustrated after being averaged across all replicas. The multi-order Laplacian operator in Eq. (1) is applied to implement the SRG. Power-law exponents are estimated using the maximum likelihood estimation approach proposed by Refs. [87, 88].

pairwise interactions follow the ER model seem to exhibit power-law behaviours after one iteration of renormalization (i.e., $k > 1$). We speculate that specific scale-invariant structures may emerge in the ER model after some high-order interactions are reduced.

The above findings can also be validated by the observations in Fig. 10, where all settings in the computational experiments are same as those in Fig. 9 except that the high-order path Laplacian operator is applied to design the SRG.

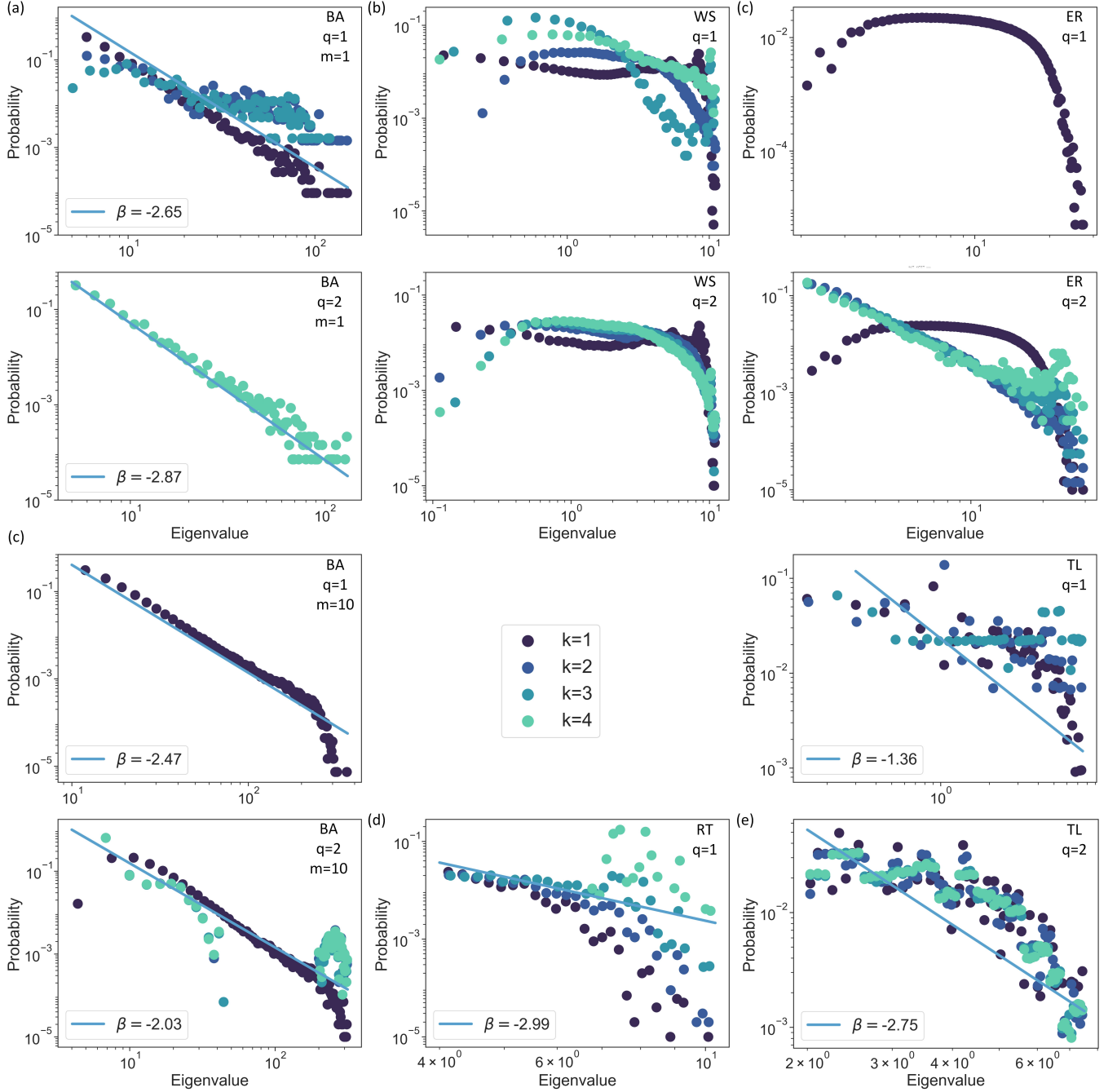


FIG. 10. The existence of the multi-order scale-invariance (Part II). (a-e) The degree distributions and the Laplacian eigenvalue spectra of different synthetic interacting systems under the transformation of the SRG are illustrated after being averaged across all replicas. The high-order path Laplacian operator in Eq. (5) is applied to implement the SRG. Power-law exponents are estimated using the maximum likelihood estimation approach proposed by Refs. [87, 88].

Appendix F: On the scaling relation and high-order effects

Here we elaborate the methodology for illustrating the scaling relation defined in Eq. (26) and the high-order effects on it when $k = 1$. In computational experiments, different types of interacting systems are generated according to their pairwise interaction properties, where each type of system has 500 replicas (i.e., realizations) and each replica consists of 1000 units.

We first derive $\beta^{(q)}(i)$ applying a maximum likelihood estimation approach proposed by Refs. [87, 88] and measure

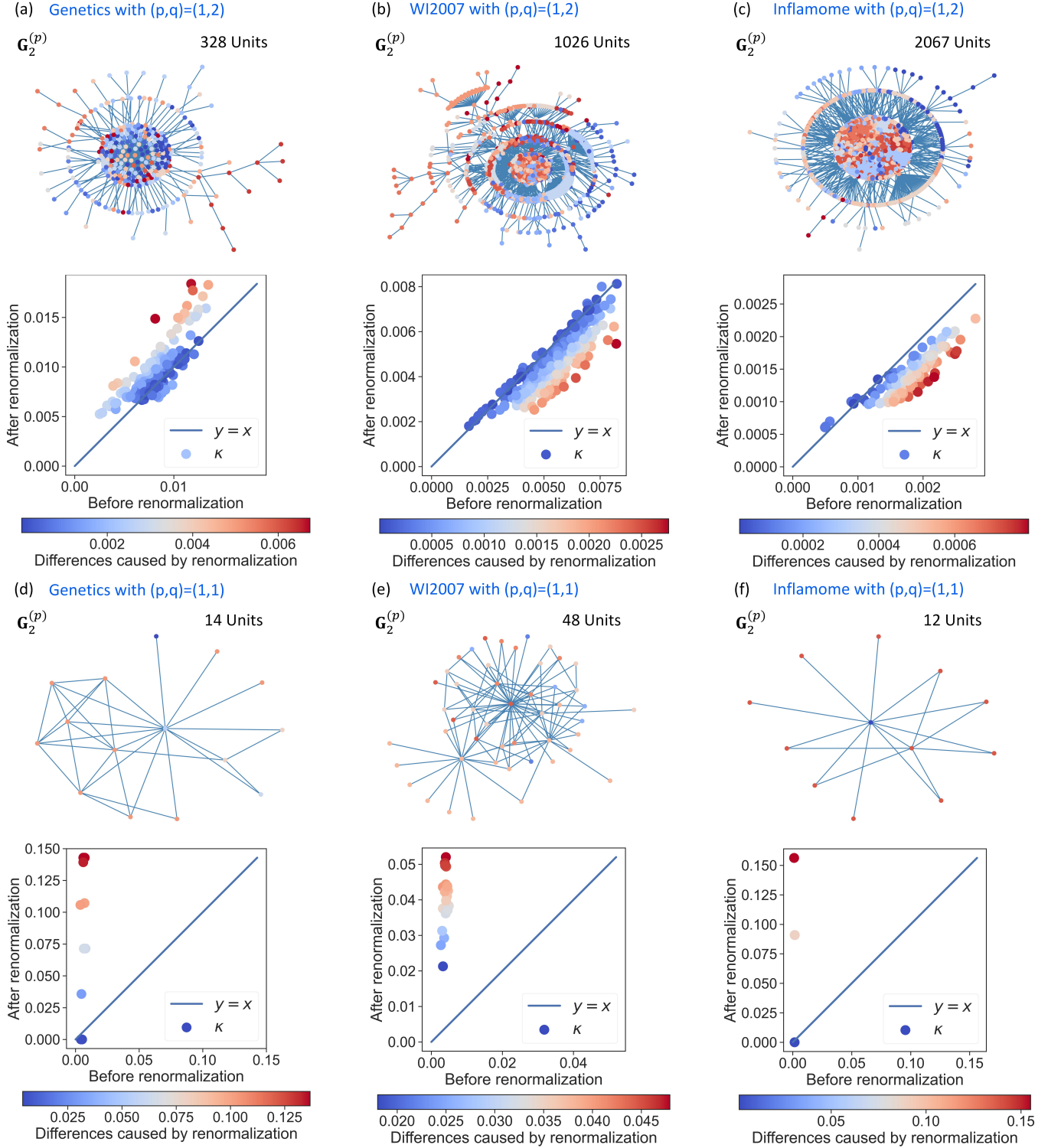


FIG. 11. The organizational structure transformed by renormalization flows. The Louvain communities of all data sets are adopted from Fig. 6 directly. (a-c) The SRG is applied to renormalize these systems with $(p, q) = (2, 1)$. The community label of each renormalized super-unit is determined according to the most frequent community label of the units aggregated into it. The values of average path distance between communities, κ , are measured before and after renormalization, whose absolute differences (i.e., see color-bars) quantify the deviation degrees from the initial organizational structures caused by renormalization. (d-f) The analysis same as (a-c) is implemented with $(p, q) = (2, 1)$.

ν using the least square method. Given each replica, we can derive the eigenvalue set $\Lambda_k^{(q)}(i)$ for its i -th cluster

and apply the maximum likelihood estimation approach [87, 88] to measure exponent $\beta^{(q)}(i)$ for the eigenvalue spectrum of this cluster such that $\beta^{(q)}(i)$ defines a power-law distribution. This estimation is implemented using the toolbox provided by Ref. [87]. After deriving $\beta^{(q)}(i)$ and $\tilde{\tau}^{(q)}(i)$ for each cluster C_i , we can calculate the value of $\tilde{\tau}^{(q)} \left\langle \frac{\beta^{(q)}(i)+1}{\tilde{\tau}^{(q)}(i)} \right\rangle_i$ for the selected replica. Parallel to this process, we can measure $\tilde{X}^{(q)}$ and $\tilde{\tau}^{(q)}$ for this replica as well.

In sum, these calculations enable us to obtain a pair of values, $(\tilde{X}^{(q)}, \tilde{\tau}^{(q)} \left\langle \frac{\beta^{(q)}(i)+1}{\tilde{\tau}^{(q)}(i)} \right\rangle_i)$, for the replica. By repeating the above calculations on all replicas, we can generate the sample sets of predictors, $\tilde{\tau}^{(q)} \left\langle \frac{\beta^{(q)}(i)+1}{\tilde{\tau}^{(q)}(i)} \right\rangle_i$, and responses, $\tilde{X}^{(q)}$, respectively. These samples can be used to implement a vanilla linear fitting $\tilde{X}^{(q)} = \tilde{\tau}^{(q)} \left\langle \frac{\beta^{(q)}(i)+1}{\tilde{\tau}^{(q)}(i)} \right\rangle_i + \nu$, where ν can be solved by the least square method. After deriving ν , we obtain a set of predictions, $\tilde{\tau}^{(q)} \left\langle \frac{\beta^{(q)}(i)+1}{\tilde{\tau}^{(q)}(i)} \right\rangle_i + \nu$, and their associated labels, $\tilde{X}^{(q)}$. By respectively averaging these predictions and labels across all replicas, we can derive the mean observations presented in Figs. 5(a-e). Meanwhile, we can quantify the departures from the scaling relation by the standard deviations of $\tilde{X}^{(q)}$ and $\tilde{\tau}^{(q)} \left\langle \frac{\beta^{(q)}(i)+1}{\tilde{\tau}^{(q)}(i)} \right\rangle_i + \nu$.

Appendix G: On organizational structure identification

Here we elaborate on the experiments of verifying whether given organizational structures can be preserved by the SRG.

Before renormalization, the communities of units are automatically detected by the Louvain community detection algorithm [66]. After every iteration of renormalization, units are aggregated into super-units according to the SRG. Here we do not define latent community structures by applying the algorithm [66] on the renormalized system again. Instead, we determine latent community structures according to unit aggregation during renormalization, where the community label of each super-unit is defined as the most frequent community label of the units aggregated into it. For instance, if six units are aggregated into a super-unit during renormalization and four of them belong to the first community, then the super-unit is defined as a member of the first community.

To characterize the organizational structure of a system with multiple communities, we can analyze the connectivity between communities in terms of normalized average path distance. Specifically, the average path distance between two communities is averaged across all path distances between the units that belong to these communities. Here the path distance between two units refers to the weighted length of the shortest paths between them (i.e., being weighted according to edge weights). A smaller average path distance suggests that two corresponding communities are closer to each other. Then, we normalize these average path distances by dividing them by the largest possible path distance (i.e., the number of units minus one). The above calculation can be implemented before and after renormalization to derive two sets of results for comparison. For instance, if the normalized average path distance between a pair of communities before renormalization is numerically similar to its counterpart after renormalization, the connectivity properties between communities are generally preserved under the transformation of the SRG.

Consistent with Ref. [38], our results in Fig. 11 suggest that the renormalized systems are not equivalent to the networks of communities (i.e., the networks where each unit is a community). Moreover, we observe qualitative similarities between apparent and latent community structures when the SRG is guided by high-order interactions (i.e., $q = 2$). These similarities can be quantitatively validated by showing how the connectivity properties (e.g., the normalized average path distances) between communities are preserved under the transformation of the SRG. For comparison, the results with $q = 1$ show that the renormalization guided by pairwise interactions, even though being applied on the same data, does not preserve community connectivity properties. On the contrary, the renormalization makes the latent community structures deviate from the apparent ones because the whole system is reduced significantly.

[1] M. Henkel, H. Hinrichsen, S. Lübeck, and M. Pleimling, *Non-equilibrium phase transitions*, Vol. 1 (Springer, 2008).

[2] S. Lübeck, Universal scaling behavior of non-equilibrium phase transitions, *International Journal of Modern Physics B* **18**, 3977 (2004).

[3] R. P. Feynman, A. R. Hibbs, and D. F. Styer, *Quantum mechanics and path integrals* (Courier Corporation, 2010).

[4] H. Kleinert, *Path integrals in quantum mechanics, statistics, and condensed matter physics* (World Scientific, 2004).

tics, polymer physics, and financial markets (World scientific, 2009).

[5] C. C. Chow and M. A. Buice, Path integral methods for stochastic differential equations, *The Journal of Mathematical Neuroscience (JMN)* **5**, 1 (2015).

[6] A. Pelissetto and E. Vicari, Critical phenomena and renormalization-group theory, *Physics Reports* **368**, 549 (2002).

[7] N. Goldenfeld, *Lectures on phase transitions and the renormalization group* (CRC Press, 2018).

[8] Y. Zhang, M. Lucas, and F. Battiston, Higher-order interactions shape collective dynamics differently in hypergraphs and simplicial complexes, *Nature Communications* **14**, 1605 (2023).

[9] M. Lucas, G. Cencetti, and F. Battiston, Multiorder laplacian for synchronization in higher-order networks, *Physical Review Research* **2**, 033410 (2020).

[10] P. Villegas, T. Gili, G. Caldarelli, and A. Gabrielli, Laplacian renormalization group for heterogeneous networks, *Nature Physics* , 1 (2023).

[11] A. R. Benson, D. F. Gleich, and J. Leskovec, Higher-order organization of complex networks, *Science* **353**, 163 (2016).

[12] R. Lambiotte, M. Rosvall, and I. Scholtes, From networks to optimal higher-order models of complex systems, *Nature physics* **15**, 313 (2019).

[13] S. Majhi, M. Perc, and D. Ghosh, Dynamics on higher-order networks: A review, *Journal of the Royal Society Interface* **19**, 20220043 (2022).

[14] F. Battiston, E. Amico, A. Barrat, G. Bianconi, G. Ferraz de Arruda, B. Franceschiello, I. Iacopini, S. Kéfi, V. Latora, Y. Moreno, *et al.*, The physics of higher-order interactions in complex systems, *Nature Physics* **17**, 1093 (2021).

[15] F. Baccini, F. Geraci, and G. Bianconi, Weighted simplicial complexes and their representation power of higher-order network data and topology, *Physical Review E* **106**, 034319 (2022).

[16] J. J. Torres and G. Bianconi, Simplicial complexes: higher-order spectral dimension and dynamics, *Journal of Physics: Complexity* **1**, 015002 (2020).

[17] M. Reitz and G. Bianconi, The higher-order spectrum of simplicial complexes: a renormalization group approach, *Journal of Physics A: Mathematical and Theoretical* **53**, 295001 (2020).

[18] A. P. Millán, J. J. Torres, and G. Bianconi, Explosive higher-order kuramoto dynamics on simplicial complexes, *Physical Review Letters* **124**, 218301 (2020).

[19] Q. F. Lotito, F. Musciotto, A. Montresor, and F. Battiston, Higher-order motif analysis in hypergraphs, *Communications Physics* **5**, 79 (2022).

[20] T. Carletti, F. Battiston, G. Cencetti, and D. Fanelli, Random walks on hypergraphs, *Physical review E* **101**, 022308 (2020).

[21] T. Carletti, D. Fanelli, and S. Nicoletti, Dynamical systems on hypergraphs, *Journal of Physics: Complexity* **1**, 035006 (2020).

[22] G. Bianconi and S. N. Dorogovtsev, The spectral dimension of simplicial complexes: a renormalization group theory, *Journal of Statistical Mechanics: Theory and Experiment* **2020**, 014005 (2020).

[23] M. T. Schaub, A. R. Benson, P. Horn, G. Lippner, and A. Jadbabaie, Random walks on simplicial complexes and the normalized hodge 1-laplacian, *SIAM Review* **62**, 353 (2020).

[24] U. Alvarez-Rodriguez, F. Battiston, G. F. de Arruda, Y. Moreno, M. Perc, and V. Latora, Evolutionary dynamics of higher-order interactions in social networks, *Nature Human Behaviour* **5**, 586 (2021).

[25] I. Iacopini, G. Petri, A. Barrat, and V. Latora, Simplicial models of social contagion, *Nature communications* **10**, 2485 (2019).

[26] G. F. De Arruda, G. Petri, F. A. Rodrigues, and Y. Moreno, Impact of the distribution of recovery rates on disease spreading in complex networks, *Physical Review Research* **2**, 013046 (2020).

[27] C. Giusti, R. Ghrist, and D. S. Bassett, Two's company, three (or more) is a simplex: Algebraic-topological tools for understanding higher-order structure in neural data, *Journal of computational neuroscience* **41**, 1 (2016).

[28] G. Petri, P. Expert, F. Turkheimer, R. Carhart-Harris, D. Nutt, P. J. Hellyer, and F. Vaccarino, Homological scaffolds of brain functional networks, *Journal of The Royal Society Interface* **11**, 20140873 (2014).

[29] L. Meshulam, J. L. Gauthier, C. D. Brody, D. W. Tank, and W. Bialek, Coarse-graining and hints of scaling in a population of 1000+ neurons, *arXiv preprint arXiv:1812.11904* (2018).

[30] G. García-Pérez, M. Boguñá, and M. Á. Serrano, Multiscale unfolding of real networks by geometric renormalization, *Nature Physics* **14**, 583 (2018).

[31] S. Bradde and W. Bialek, Pca meets rg, *Journal of statistical physics* **167**, 462 (2017).

[32] V. Lahoche, D. O. Samary, and M. Tamaazousti, Generalized scale behavior and renormalization group for data analysis, *Journal of Statistical Mechanics: Theory and Experiment* **2022**, 033101 (2022).

[33] M. Zheng, A. Allard, P. Hagmann, Y. Alemán-Gómez, and M. Á. Serrano, Geometric renormalization unravels self-similarity of the multiscale human connectome, *Proceedings of the National Academy of Sciences* **117**, 20244 (2020).

[34] C. Song, S. Havlin, and H. A. Makse, Self-similarity of complex networks, *Nature* **433**, 392 (2005).

[35] C. Song, S. Havlin, and H. A. Makse, Origins of fractality in the growth of complex networks, *Nature physics* **2**, 275 (2006).

[36] K.-I. Goh, G. Salvi, B. Kahng, and D. Kim, Skeleton and fractal scaling in complex networks, *Physical review letters* **96**, 018701 (2006).

[37] J. S. Kim, K.-I. Goh, B. Kahng, and D. Kim, Fractality and self-similarity in scale-free networks, *New Journal of Physics* **9**, 177 (2007).

[38] D. Gfeller and P. De Los Rios, Spectral coarse graining of complex networks, *Physical review letters* **99**, 038701 (2007).

[39] K. Klemm and V. M. Eguiluz, Growing scale-free networks with small-world behavior, *Physical Review E* **65**, 057102 (2002).

[40] D. Krioukov, F. Papadopoulos, M. Kitsak, A. Vahdat, and M. Boguná, Hyperbolic geometry of complex networks, *Physical Review E* **82**, 036106 (2010).

[41] M. Matsumoto, G. Tanaka, and A. Tsuchiya, The renormalization group and the diffusion equation, *Progress of Theoretical and Experimental Physics* **2021**, 023B02 (2021).

[42] M. De Domenico and J. Biamonte, Spectral entropies as

information-theoretic tools for complex network comparison, *Physical Review X* **6**, 041062 (2016).

[43] P. Villegas, A. Gabrielli, F. Santucci, G. Caldarelli, and T. Gili, Laplacian paths in complex networks: Information core emerges from entropic transitions, *Physical Review Research* **4**, 033196 (2022).

[44] J. S. Andrade Jr, H. J. Herrmann, R. F. Andrade, and L. R. Da Silva, Apollonian networks: Simultaneously scale-free, small world, euclidean, space filling, and with matching graphs, *Physical review letters* **94**, 018702 (2005).

[45] S. N. Dorogovtsev, A. V. Goltsev, and J. F. F. Mendes, Pseudofractal scale-free web, *Physical review E* **65**, 066122 (2002).

[46] S. Hwang, C.-K. Yun, D.-S. Lee, B. Kahng, and D. Kim, Spectral dimensions of hierarchical scale-free networks with weighted shortcuts, *Physical Review E* **82**, 056110 (2010).

[47] R. Albert and A.-L. Barabási, Statistical mechanics of complex networks, *Reviews of modern physics* **74**, 47 (2002).

[48] A.-L. Barabási, Scale-free networks: a decade and beyond, *science* **325**, 412 (2009).

[49] R. K. Pathria, *Statistical mechanics* (Elsevier, 2016).

[50] C. J. Thompson, *Mathematical statistical mechanics* (Princeton University Press, 2015).

[51] A. Cheng, P. Sun, and Y. Tian, A toolbox for simplex path integral and renormalization group for high-order interactions (2023), open source codes available at <https://github.com/AohuaCheng/Simplex-Renormalization-Group>.

[52] M. Newman, *Networks* (Oxford university press, 2018).

[53] M. E. Newman, A.-L. E. Barabási, and D. J. Watts, *The structure and dynamics of networks*. (Princeton university press, 2006).

[54] M. E. Newman *et al.*, Random graphs as models of networks, *Handbook of graphs and networks* **1**, 35 (2003).

[55] F. Bullo, *Lectures on network systems*, Vol. 1 (Kindle Direct Publishing, 2020).

[56] S. Hu and L. Qi, The laplacian of a uniform hypergraph, *Journal of Combinatorial Optimization* **29**, 331 (2015).

[57] J. Zhou, L. Sun, W. Wang, and C. Bu, Some spectral properties of uniform hypergraphs, *arXiv preprint arXiv:1407.5193* (2014).

[58] D. Horak and J. Jost, Spectra of combinatorial laplace operators on simplicial complexes, *Advances in Mathematics* **244**, 303 (2013).

[59] Y. Chebbi, The discrete laplacian of a 2-simplicial complex, *Potential Analysis* **49**, 331 (2018).

[60] A. Ghavasieh, M. Stella, J. Biamonte, and M. De Domenico, Unraveling the effects of multi-scale network entanglement on empirical systems, *Communications Physics* **4**, 129 (2021).

[61] A. Ghavasieh, S. Bontorin, O. Artíme, N. Verstraete, and M. De Domenico, Multiscale statistical physics of the pan-viral interactome unravels the systemic nature of sars-cov-2 infections, *Communications Physics* **4**, 83 (2021).

[62] P. Moretti and M. Zaiser, Network analysis predicts failure of materials and structures, *Proceedings of the National Academy of Sciences* **116**, 16666 (2019).

[63] D. J. Watts and S. H. Strogatz, Collective dynamics of ‘small-world’ networks, *nature* **393**, 440 (1998).

[64] P. Erdős, A. Rényi, *et al.*, On the evolution of random graphs, *Publ. Math. Inst. Hung. Acad. Sci* **5**, 17 (1960).

[65] N. Simonis, J.-F. Rual, A.-R. Carvunis, M. Tasan, I. Lemmens, T. Hirozane-Kishikawa, T. Hao, J. M. Sahalie, K. Venkatesan, F. Gebreab, *et al.*, Empirically controlled mapping of the *caenorhabditis elegans* protein-protein interactome network, *Nature methods* **6**, 47 (2009).

[66] V. D. Blondel, J.-L. Guillaume, R. Lambiotte, and E. Lefebvre, Fast unfolding of communities in large networks, *Journal of statistical mechanics: theory and experiment* **2008**, P10008 (2008).

[67] S. Fortunato, Community detection in graphs, *Physics reports* **486**, 75 (2010).

[68] J. Reichardt and S. Bornholdt, Statistical mechanics of community detection, *Physical review E* **74**, 016110 (2006).

[69] A. Clauset, M. E. Newman, and C. Moore, Finding community structure in very large networks, *Physical review E* **70**, 066111 (2004).

[70] M. Koch-Janusz and Z. Ringel, Mutual information, neural networks and the renormalization group, *Nature Physics* **14**, 578 (2018).

[71] P. M. Lenggenhager, D. E. Gökmen, Z. Ringel, S. D. Huber, and M. Koch-Janusz, Optimal renormalization group transformation from information theory, *Physical Review X* **10**, 011037 (2020).

[72] H.-Y. Hu, S.-H. Li, L. Wang, and Y.-Z. You, Machine learning holographic mapping by neural network renormalization group, *Physical Review Research* **2**, 023369 (2020).

[73] N. Tishby, F. C. Pereira, and W. Bialek, The information bottleneck method, *arXiv preprint physics/0004057* (2000).

[74] A. A. Alemi, I. Fischer, J. V. Dillon, and K. Murphy, Deep variational information bottleneck, *arXiv preprint arXiv:1612.00410* (2016).

[75] A. M. Saxe, Y. Bansal, J. Dapello, M. Advani, A. Kolchinsky, B. D. Tracey, and D. D. Cox, On the information bottleneck theory of deep learning, *Journal of Statistical Mechanics: Theory and Experiment* **2019**, 124020 (2019).

[76] G. Chechik, A. Globerson, N. Tishby, and Y. Weiss, Information bottleneck for gaussian variables, *Advances in Neural Information Processing Systems* **16** (2003).

[77] A. G. Kline and S. E. Palmer, Gaussian information bottleneck and the non-perturbative renormalization group, *New journal of physics* **24**, 033007 (2022).

[78] Y. Tian, H. Hou, G. Xu, Z. Zhang, and P. Sun, Network comparison via encoding, decoding, and causality, *Physical Review Research* **5**, 033129 (2023).

[79] S. Gao, G. Ver Steeg, and A. Galstyan, Efficient Estimation of Mutual Information for Strongly Dependent Variables, in *Proceedings of the Eighteenth International Conference on Artificial Intelligence and Statistics*, Proceedings of Machine Learning Research, Vol. 38, edited by G. Lebanon and S. V. N. Vishwanathan (PMLR, San Diego, California, USA, 2015) pp. 277–286.

[80] G. V. Steeg, Non-parametric entropy estimation toolbox (2022), open source codes available at <https://github.com/gregversteeg/NPEET/>.

[81] G. Cimini, T. Squartini, F. Saracco, D. Garlaschelli, A. Gabrielli, and G. Caldarelli, The statistical physics of real-world networks, *Nature Reviews Physics* **1**, 58 (2019).

- [82] Y. Tian, Z. Tan, H. Hou, G. Li, A. Cheng, Y. Qiu, K. Weng, C. Chen, and P. Sun, Theoretical foundations of studying criticality in the brain, *Network Neuroscience* **6**, 1148 (2022).
- [83] L. Meshulam, J. L. Gauthier, C. D. Brody, D. W. Tank, and W. Bialek, Coarse graining, fixed points, and scaling in a large population of neurons, *Physical review letters* **123**, 178103 (2019).
- [84] A. Cavagna, L. Di Carlo, I. Giardina, L. Grandinetti, T. S. Grigera, and G. Pisegna, Dynamical renormalization group approach to the collective behavior of swarms, *Physical Review Letters* **123**, 268001 (2019).
- [85] A. Chaudhuri and W. Hu, A fast algorithm for computing distance correlation, *Computational statistics & data analysis* **135**, 15 (2019).
- [86] A. Kraskov, H. Stögbauer, and P. Grassberger, Estimating mutual information, *Physical review E* **69**, 066138 (2004).
- [87] J. Alstott, E. Bullmore, and D. Plenz, powerlaw: a python package for analysis of heavy-tailed distributions, *PloS one* **9**, e85777 (2014).
- [88] A. Clauset, C. R. Shalizi, and M. E. Newman, Power-law distributions in empirical data, *SIAM review* **51**, 661 (2009).